

Accepted Manuscript

Novel SERMs based on 3-aryl-4-aryloxy-2H-chromen-2-one skeleton - A possible way to dual ER α /VEGFR-2 ligands for treatment of breast cancer

Guoshun Luo, Xinyu Li, Guoqing Zhang, Chengzhe Wu, Zhengpu Tang, Linyi Liu, Qidong You, Hua Xiang



PII: S0223-5234(17)30697-9

DOI: [10.1016/j.ejmech.2017.09.015](https://doi.org/10.1016/j.ejmech.2017.09.015)

Reference: EJMECH 9730

To appear in: *European Journal of Medicinal Chemistry*

Received Date: 18 July 2017

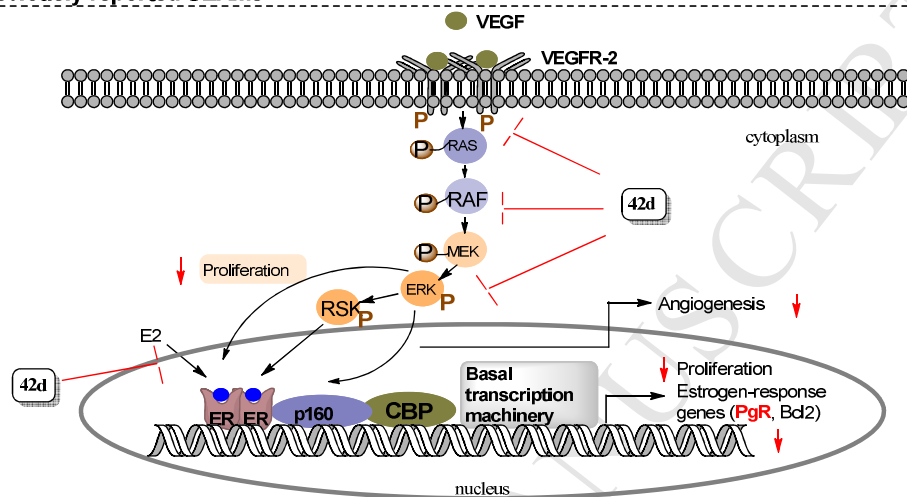
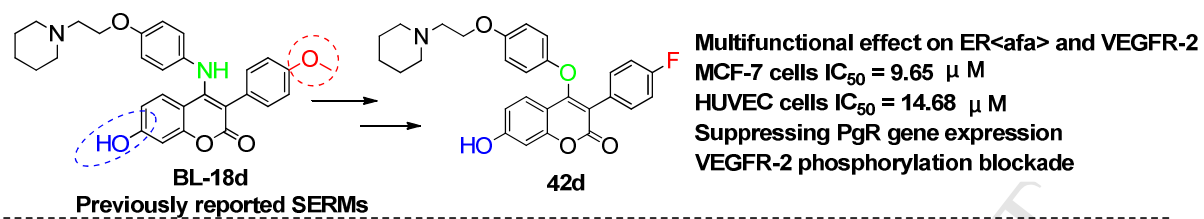
Revised Date: 24 August 2017

Accepted Date: 10 September 2017

Please cite this article as: G. Luo, X. Li, G. Zhang, C. Wu, Z. Tang, L. Liu, Q. You, H. Xiang, Novel SERMs based on 3-aryl-4-aryloxy-2H-chromen-2-one skeleton - A possible way to dual ER α /VEGFR-2 ligands for treatment of breast cancer, *European Journal of Medicinal Chemistry* (2017), doi: 10.1016/j.ejmech.2017.09.015.

This is a PDF file of an unedited manuscript that has been accepted for publication. As a service to our customers we are providing this early version of the manuscript. The manuscript will undergo copyediting, typesetting, and review of the resulting proof before it is published in its final form. Please note that during the production process errors may be discovered which could affect the content, and all legal disclaimers that apply to the journal pertain.

Graphical abstract



Novel SERMs based on 3-aryl-4-aryloxy-2H-chromen-2-one Skeleton - A Possible Way to Dual ER α /VEGFR-2 Ligands for treatment of Breast cancer

Guoshun Luo^a, Xinyu Li^a, Guoqing Zhang^a, Chengzhe Wu^a, Zhengpu Tang^a, Linyi Liu^a, Qidong You^a, Hua Xiang^{a*}

^aJiangsu Key Laboratory of Drug Design and Optimization, China Pharmaceutical University, 24 Tongjiaxiang, Nanjing 210009, PR China

* Corresponding author. Tel.: +86 025 83271096; Fax: +86 025 83271096 (H. Xiang).

E-mail addresses: xianghua@cpu.edu.cn (H. Xiang)

Abstract

There is considerable interest in developing new SERMs as multifunctional agents in women's health. Development of dual selective estrogen receptor modulators/VEGFR-2 inhibitors (SERMs/V-2I) has been an attractive strategy for the discovery of new breast cancer therapeutic agents. Our previous efforts led to the preparation of a series of 3-aryl-4-anilino-2H-chromen-2-ones endowed with potent estrogen receptor binding affinity and anti-proliferative efficacy. In this study, various structurally related 3-aryl-4-anilino/aryloxy-2H-chromen-2-one analogues were rationally designed, synthesized and evaluated as a new chemo-type of dual ER α and VEGFR-2 inhibitors. Most of the derivatives exhibited potent activities in both enzymatic and cellular assays. SAR investigation revealed that introducing of bioisosteric O atom at the C-4 position of coumarin scaffold is beneficial to improve the inhibitory potency, especially in ER α binding affinity assay. Furthermore, most of the piperidyl substituted compounds showed better inhibitory activity against MCF-7 and Ishikawa cells than lead compounds **BL-18d**, tamoxifen and Vandetanib. Optimization of the hit compound, identified in an ER α binding affinity assay, led to compound **42d**, exhibiting an IC₅₀ for ER α binding affinity of 2.19 μ M while retaining an excellent inhibition on VEGFR-2 as well as a potent suppression on the growth of angiogenesis-related cells. In RT-PCR assay, **42d** exerted significantly antiestrogenic property via suppressing the expression of progesterone receptor (PgR) mRNA in MCF-7 cells, which was consistent with the ER α antagonistic property of a selective estrogen receptor modulator. Further mechanism investigation demonstrated that compound **42d** could inhibit the activation of VEGFR-2 and subsequent signaling transduction of Raf-1/MAPK/ERK pathway in MCF-7 cells. All these results together with molecular modeling studies open a new avenue for the development of multifunctional agents targeting ER α and VEGFR-2 in the therapy of some breast cancers.

Keywords: Estrogen receptor; VEGFR-2; Coumarin; Anti-breast cancer; Docking studies.

1. Introduction

Breast cancer is the most prevalent form of cancer diagnosed in women worldwide, with an incidence that rises dramatically with age. An estimated 1.7 million women will be diagnosed with breast cancer in 2020 - a 26% increase from current levels [1]. Estrogens are a group of steroid hormones and key regulators of growth, differentiation and function of the female reproductive organs including the breast, uterus and ovaries [2]. The biological actions of estrogens are mediated through intracellular transcription factors called estrogen receptors (ER) which belong to the nuclear receptor superfamily. Estrogen receptors (ER) mediate estrogen activity in many important physiological processes and play vital roles in the development of therapeutic agents for breast cancer treatment [3, 4]. Despite a remarkable increase in the depth of our understanding and management of breast cancer in the past 50 years, the disease remains a significant public health problem worldwide and poses significant challenges [5].

It is well known that approximately 70% of human breast cancers are hormone-dependent and ER α -positive [6]. Endocrine therapy which aims to block the ER transcription effect is regarded as an effective treatment. Thus ER α has provided an ideal pharmaceutical target and a lot of ER α ligands have been developed as antagonists against ER α positive breast cancer [7]. Selective estrogen receptor modulators (SERMs) are a special group of ligands which act as antagonists in breast tissue but agonists in other tissues such as cardiovascular system and bone [8, 9]. Due to their special action mode, SERMs remain as important anti-breast cancer agents with benefits in cardiovascular system and maintaining bone density compared with aromatase inhibitors and pure anti-estrogens [10, 11]. Tamoxifen (a SERM, **1a**), containing a triphenylethylene scaffold and a basic side chain, was the first SERM approved for the treatment of breast cancer and have provided invaluable treatments for a number of patients [12-14]. Its active metabolite, 4-hydroxy [4-OH] tamoxifen **1b**, exhibits a high binding affinity for the ER. Since then, many SERMs with various scaffolds mimicking Tamoxifen have been developed for the treatment or prevention of breast cancer [15, 16]. Many alternative scaffolds for ER modulators have also been reported, e.g., the naphthalene ring system (**3**), benzopyran-based analogue (ormeloxifene, **4**), dihydrobenzoxathiin platform (**5**) and coumarin-based benzopyranone analogues (**6**, **BL-16d** and **BL-18d**) (Figure 1) [17-21].

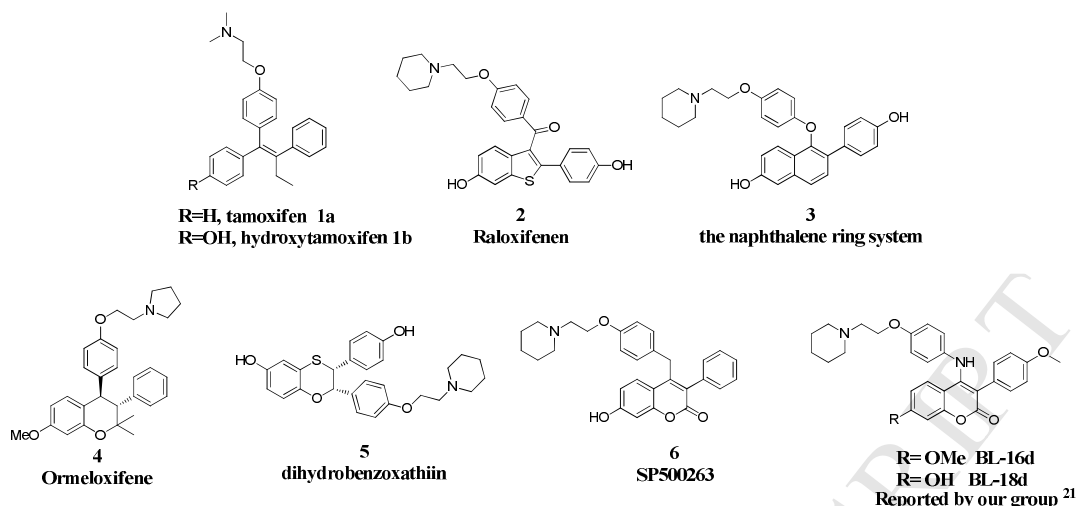


Figure 1. Previously reported selective estrogen receptor modulators (SERMs)

Although SERMs have improved the outcome for ER α positive breast cancer patients, unfortunately, undesired side effects severely limit their therapeutic use. For instance, long-term treatment of Tamoxifen increases the occurrence of endometrial cancer due to their partial estrogenic activity on the endometrium [22]. Intrinsic and acquired drug resistance is another common deficiency that limits the use of SERMs, in which breast tumors become refractory to endocrine therapies and relapse [23, 24]. Therefore, there is still a need for developing new ER ligands with better therapeutic effect.

Recently, intensive interest in discovery of novel anti-breast cancer drugs based on different mechanisms of action is highlighted by the pursuit of multiple ligands acting at multiple biomolecular targets. These multifunctional conjugates may exert favorable advantages of improved efficacy and lower incidence of side effects [25]. Several attempts have been made to improve efficacy through coupling a potent ER ligand to a second component, such as an antimetabolite agent (E2-nucleoside conjugate **7**) [26], alkylating agent (E2-chlorambucil conjugate **8**) [27], tubulin agent (dual ER-tubulin agent **9**) [28], histone deacetylase (HDAC) inhibitor (dual ER-HDAC agent **10**) [29], and aromatase agent (dual ER-aromatase agent **11**) [30] (Fig. 2A).

However, with the development of acquired resistance in breast and endometrial tumors it is axiomatic that selective estrogen receptor modulators (SERMs, tamoxifen and raloxifene) stimulated tumors must induce angiogenesis to grow [31]. Tumor angiogenesis is vital to cancer growth, metastasis and invasion, and thus represents an attractive therapeutic target [32]. Vascular endothelial growth factor receptor-2 (VEGFR-2) is a member of the receptor tyrosine kinase (RTK) family and the predominant effector of VEGF/VEGFR signaling in promoting angiogenesis in cancer [33]. The phosphorylation of VEGFR-2 will activate the Raf-1/MAPK/ERK signaling which is very important

for cell proliferation, migration, invasion, and angiogenesis [34]. Moreover, studies have revealed that the Raf-1/MAPK/ERK interplays with ER in regulating estrogen-dependent gene expression and is widely observed in the endocrine resistance [35, 36]. Monotherapy of VEGFR-2 inhibitors were reported in the treatment of breast cancer but are not sufficient as single therapy [37]. We thus hypothesize that building VEGFR-2 inhibitory activity into SERMs could be an effective way to improve the efficacy and decrease the side effects associated with them. Indeed, a combination of Tamoxifen with Brivanib, a VEGFR-2 inhibitor, was recently reported not only to maximize therapeutic efficacy but also to retard SERM resistant tumor growth [31]. Moreover, 2, 3-diaryl isoquinolinone (**12**) and 6-aryl-indenoisoquinolone (**13**) were reported by our group as multiple ligands of ER α and VEGFR-2, which showed inhibition on both targets and potent anti-cancer activity [38, 39] (Fig. 2B). These inspiring evidences suggest that simultaneous ER and VEGFR-2 inhibition could be a promising approach in breast cancer therapy.

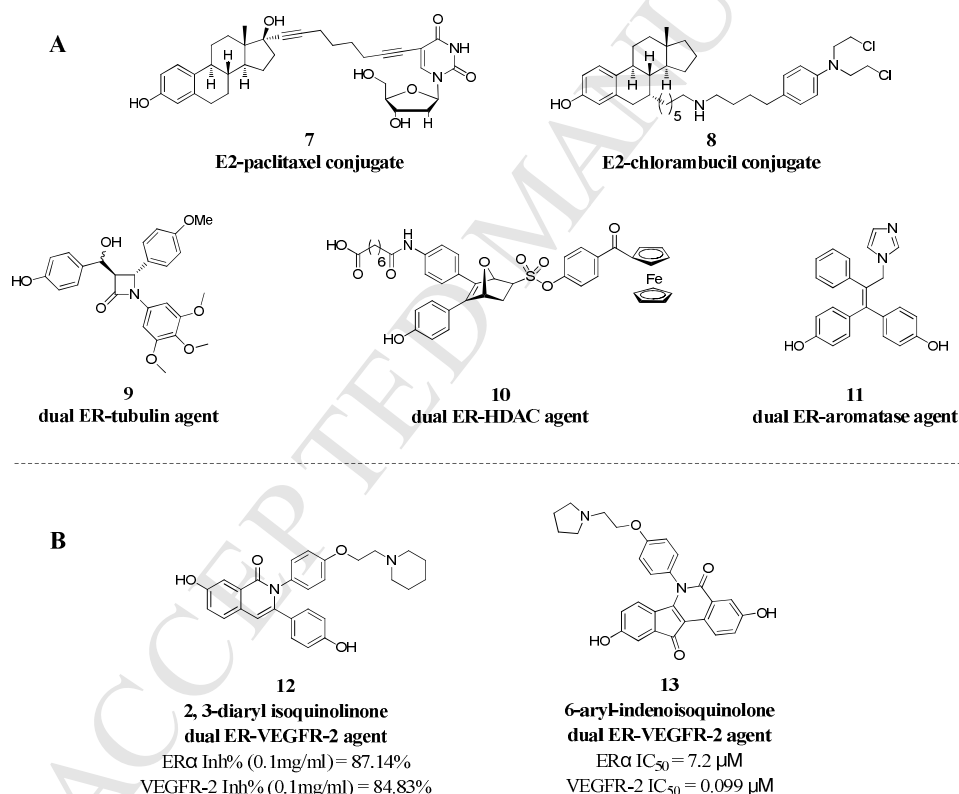


Figure 2. (A) Previously referenced dual-acting ER ligand conjugates (B) multiple ligands of ER α and VEGFR-2 together with outstanding biological results reported by our group previously

Coumarins constitute an important class of pharmacologically active scaffolds known to exert versatile biological activities including anticancer [40-43], anti-HIV [44], anti-microbial [45], and anti-inflammatory activity [46]. The therapeutic applications of coumarins depend upon the pattern of substitution and have attracted intense interest in recent years due to their diverse pharmacological

properties [47]. Among these properties, their anticancer effects were the most extensively examined [48, 49]. Studies have revealed the mechanism behind the anticancer effect of coumarin analogs which include anti-angiogenesis and induction of apoptosis independently [50-53]. As the current strategies in cancer drug development shifted toward the multiple mechanistic approach [54], such validation of structure-activity relationship of coumarins with respect to angiogenesis and anti-proliferation activity leads to dual-action anti-tumor activities deserve to be investigated.

Previously, we have prepared a series of novel SERMs based on 3-aryl-4-anilino-2H-chromen-2-one core, of which the piperidyl substituted analogues **BL-16d** (with OMe at C-7 position of the coumarin nucleus) and **BL-18d** (with OH at C-7 position of the coumarin nucleus) demonstrated strong ER α binding affinities and excellent anti-proliferative activities against MCF-7 and Ishikawa cells [21]. As an extension of our study in the development of novel SERMs with high therapeutic index, here we adopted 3, 4-disubstituted-2H-chromen-2-ones (**BL-18d** and **BL-16d**) as promising lead compounds in this study for further optimized as novel anti-breast cancer agents with multiple mechanistic profiles.

2. Structure-Based Drug Design

Encouraged by the promising research results mentioned above, our further efforts focused on discovery of novel coumarin-based anti-breast cancer agents dual targeting ER α and VEGFR-2. To rationalize the modification of 3, 4-disubstituted-2H-chromen-2-one, docking study of **BL-18d** with ER α active site was carried out by CDOCKER protocol in Discovery studio 3.0 (PDB: 3ERT). As shown in Figure 3A, the hydrogen bond interactions of lead compound's 7-OH with Glu353 and Arg394 and 4'-OMe with His524 play important roles in stabilizing the binding mode of **BL-18d** to ER α . Furthermore, It has been indicated that that an oxygen linker confers a substantial increase in estrogen antagonist potency [55]. Our first exploration focused on the biological effect of the bridging atoms between the phenyl and coumarin moieties, in addition to the established NH linker, bioisosteric group O atom was also employed. Subsequently, two more groups (F and OH) were further attached to C-4' position of 3-phenyl substituent. Studies showed that incorporation of fluorine to a bioactive molecule causes minimal steric alterations and, hence, can facilitate interactions of that biomolecule with enzyme active sites, receptor recognition sites and other biological systems [56, 57]. Additionally, these hydroxyl containing derivatives bearing more hydrogen bond donors could retain essential hydrogen bonds with essential amino acid residues of targeted ER α receptor and VEGFR-2 enzyme. Finally, various medium size tertiary amines including dimethyl amine, diethyl amine, pyrrolidinyl and piperidyl were incorporated to terminal basic side chain to obtain diverse derivatives.

In the past decades, a number of potent VEGFR inhibitors including Vandetanib, Vatalanib (PTK787) and Cabotantinib have been identified and brought to clinical trials in the treatment of

angiogenesis-related diseases [58, 59]. The essential pharmacophoric features in the representative VEGFR-2 inhibitors (Figure 3B) include fused aromatic system and substituted aniline or aryloxy moiety which target the kinase domain of VEGFR. Recently, several coumarin-type compounds were reported to block angiogenesis by inhibiting endothelial cell growth and have attracted considerable attention as antitumor agents [52, 53]. In this context, 3, 4-disubstituted-2H-chromen-2-one containing fused aromatic ring and solvent side chain region in particular emerged as an interesting scaffold for designing VEGFR inhibitors. On the other hand, the structural optimization was also guided and corroborated by molecular docking of a putative compound **17d** ($R^1=R^2=OH$) into the VEGFR-2 ligand binding domain (PDB: 1YWN; Figure 3C). Analysis of the molecular docking results revealed both hydrogen bond interactions and Pi-Pi interactions of the coumarin moiety in the bind site formed by critical amino acid residues phe916 (6.30 Å), Cys917 (2.62 and 2.96 Å) and Lys866 (2.78 Å), which we believe will contribute, at least in part, to VEGFR-2 inhibition. Overall, the design strategy and structures of the title compounds were represented in Fig. 3D.

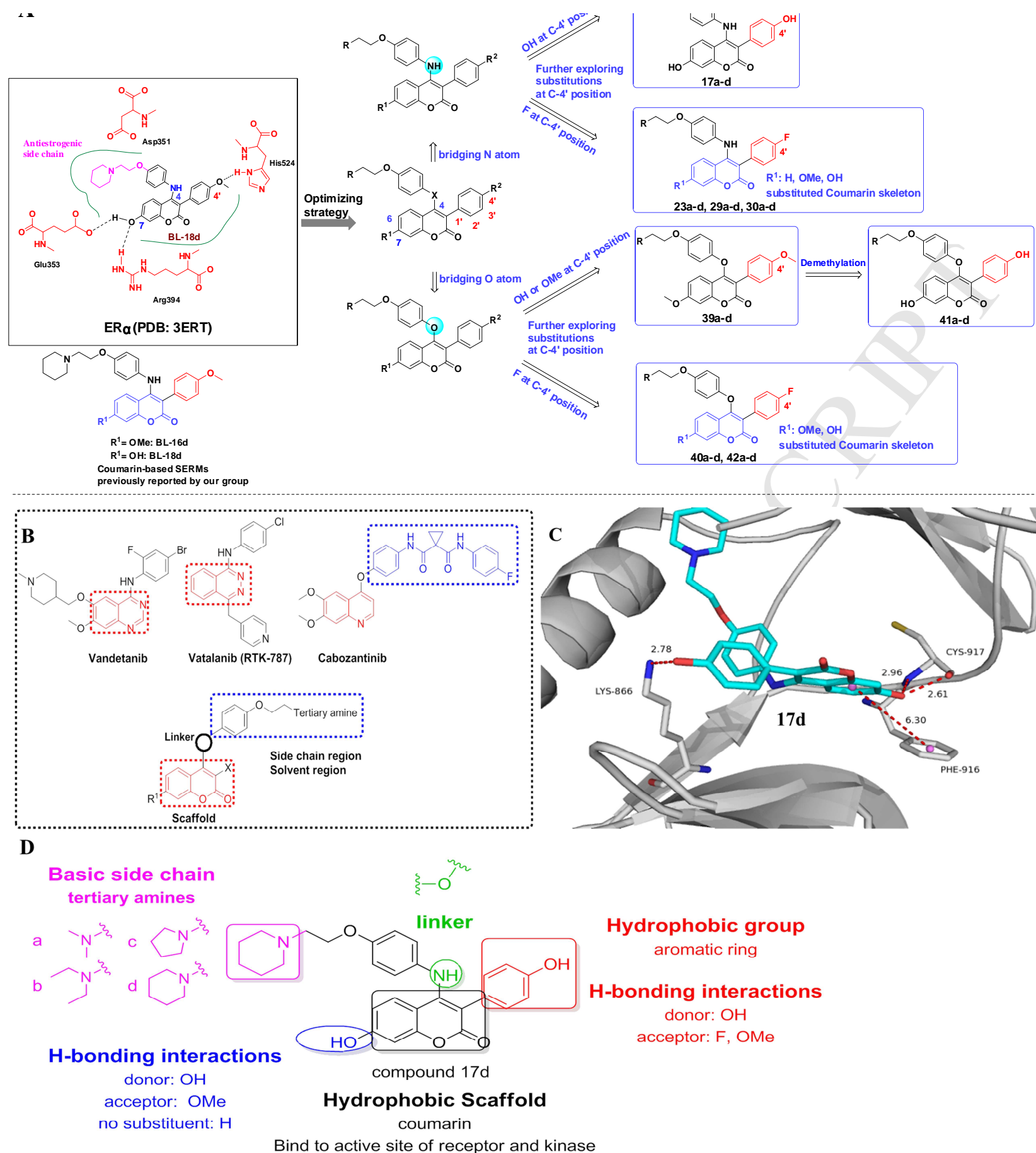


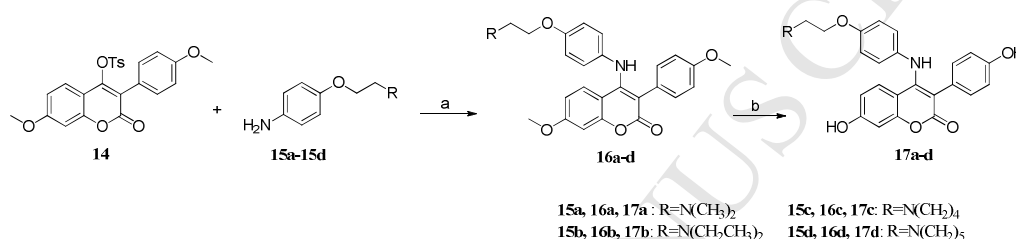
Figure 3. The rationally design of targeted compounds based on 3-aryl-4-anilino/aryloxy-2H-chromen-2-one scaffold. (A) Schematic representation of the catalytic pocket of ER α and the chemical modulation strategy. (B) Previously reported VEGFR-2 inhibitor and the design of novel inhibitor for VEGFR-2 kinase (C) Docking analysis of a putative compound **17d** within active site of VEGFR-2 (for clarity, only interacting residues are labeled. Hydrogen-bonding and hydropholic interactions are shown by red dashes). (D) Schematic representation showing the overall designing strategy of dual ER α and VEGFR-2 ligands.

Herein, we describe the synthesis of 32 novel coumarin-based analogs, preliminary pharmacological data from receptor binding and cellular assays, and mechanism investigation on Raf-1/MAPK/ERK pathway. This allowed a straightforward evaluation of ER α binding affinity, anti-proliferative potency, antiangiogenic activity, anti-estrogenic property as well as the expression of essential proteins from VEGFR-2/Raf-1/MAPK/ERK signaling pathway. Molecule docking was further carried out for ER α and VEGFR-2 in order to explore the potential binding mode of the novel dual-action inhibitors.

3. Results and discussion

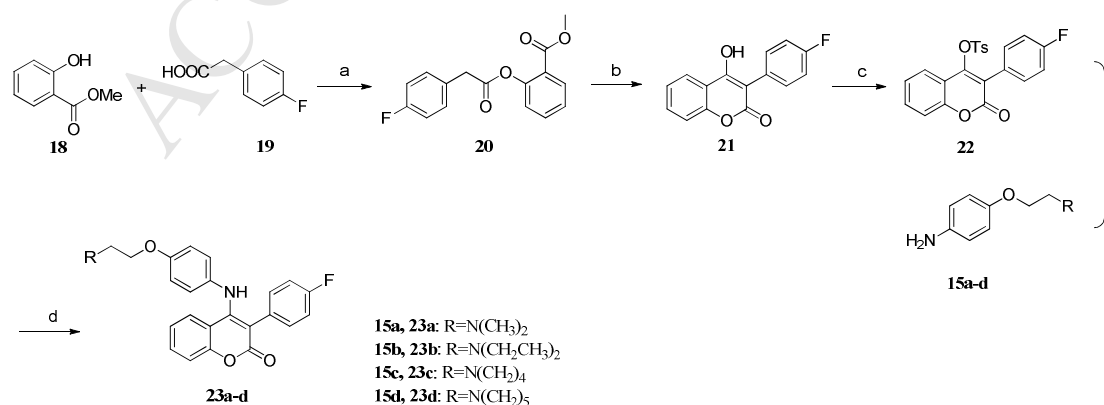
3.1 Chemistry.

The synthetic route of two hydroxyl containing 3-aryl-4-anilino-2H-chromen-2-one derivatives **17a-d** was shown in Scheme 1. This synthetic strategy utilized a key starting material, 7-methoxy-3-(4-methoxyphenyl)-2-oxo-2H-chromen-4-yl 4-methylbenzenesulfonate (**14**), which was synthesized through a facile route previously reported by our group [43]. Nucleophilic substitution of **14** with previously synthesized 4-[(2-aminoethoxy)]-substituted anilines **15a-d** [21] afforded compounds **16a-d**, which were then converted to the final compounds **17a-d** through demethylation.



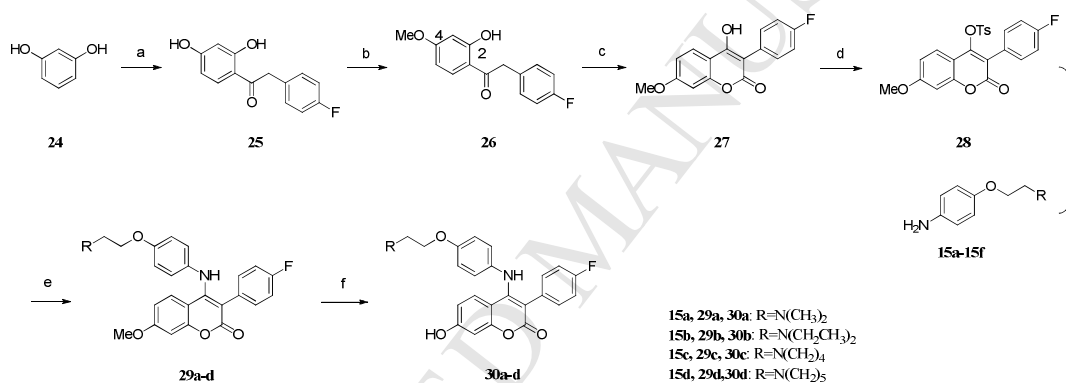
Scheme 1. Synthetic routes of **17a-d**. Reagents and conditions: (a) K₂CO₃, EtOH, 75 °C, 3 h; (b) BBr₃, CH₂Cl₂, rt, 12 h.

The design and synthesis of 4'-fluorine substituted 3-aryl-4-anilino-2H-chromen-2-one analogues **23a-d**, **32a-d** and **34a-d** were successfully processed following the previously reported procedures [43]. The synthetic sequence of **23a-d** began with the commercially available methyl salicylate **18**, which were easily converted to the esterified product **20** (Scheme 2). The following cyclized compound **21** was prepared from corresponding intermediate **20** via intramolecular Claisen condensation. Further treatment of **21** with paratoluensulfonyl chloride provided sulfonate precursor which were then coupled with various 4-[(2-aminoethoxy)]-substituted anilines **15a-d** via the nucleophilic substitution to yield the target compounds **23a-d** in good to moderate yields.



Scheme 2. Synthetic routes of **23a-d**. Reagents and conditions: (a) POCl₃, pyridine, 0-10 °C, 2 h; (b) KOH, pyridine, rt, 4 h; (c) TsCl, Et₃N, dry DCM, rt, 0.5 h; (d) arylamines, K₂CO₃, EtOH, 75 °C, 2-3 h.

The synthesis of compounds **29a-d** and **30a-d** is shown in Scheme 3. Briefly, resorcinol reacted with 4-hydroxybenzoic acid to yield benzophenone **25** under Friedel-Crafts reaction conditions, which was then converted to the corresponding 4-methoxy deoxybenzoin **26** through alkylation of 4-hydroxyl with methanol via Mitsunobu reaction. Further treatment of **26** with diethyl carbonate (DEC)/NaH in reflux toluene gave cyclized compound **27**, which were then subjected to an esterification reaction in the presence of TsCl and TEA in DCM to provide the key intermediates **28**. Subsequently, the introduction of different substituents **15a-d** on the C-4 position of **28** provided targeted compounds **29a-d**. The removal of the methyl group of compounds **29a-d** with BBr₃ in DCM produced desired analogues **30a-d**.

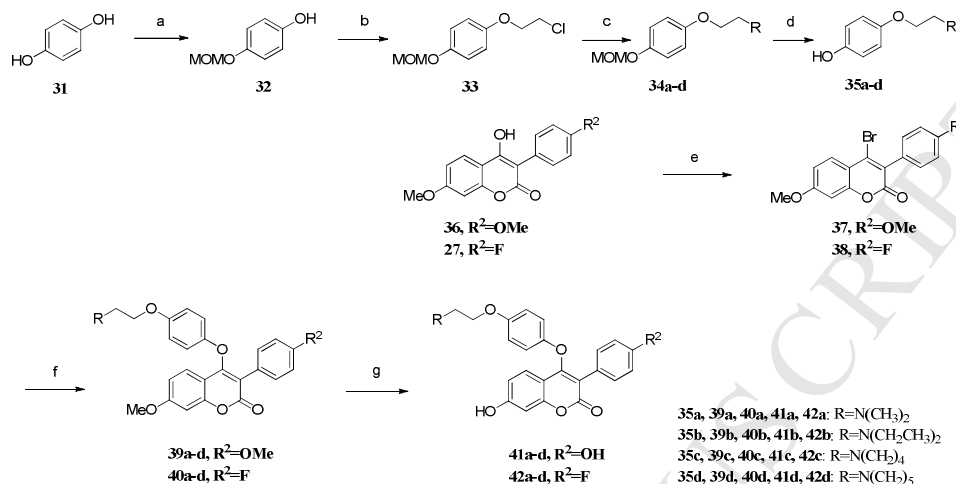


Scheme 3. Synthetic routes of **29a-d** and **30a-d**. Reagents and conditions: (a) BF₃-OEt₂, 85 °C, 2.5 h; (b) MeOH, PPh₃, DIAD, THF, 0 °C-rt, 0.5 h; (c) NaH, DEC, 120 °C, 2 h; (d) TsCl, Et₃N, dry DCM, 0.5 h; (e) arylamines, K₂CO₃, EtOH, 75 °C, 2-3 h; (f) BBr₃, CH₂Cl₂, rt, 12 h.

Subsequently, we designed and synthesized the 4-O-linked 3-aryl-4- aryloxy-2H-chromen-2-one derivatives to further investigate the effects of the bridging O atom between the phenyl and coumarin moieties on biological activity. The Synthetic routes of the 4-[(2-aminoethoxy)]-substituted phenols **35a-d** and the desired 4-anilino-3-aryl-2H-chromen-2-ones **39a-d**, **40a-d**, **41a-d** and **42a-d** are outlined in Scheme 4. The 4-[(2-aminoethoxy)]-substituted phenols **35a-d** were obtained in four steps involving: i) selective etherification of hydroquinone **31** with methoxymethyl chloride; ii) reaction of the resulting mon-etherified product **32** with 1, 2-dichloroethane; iii) treatment of the 2-chloroethyl derivative **33** with selected amines; and, finally iv) removal of the methoxymethyl group in the aminated derivatives **34a-d**.

The bromination of preexisting 4-hydroxy coumarins **36** [43] and **27** with excess phosphorus oxybromide was carried out to give the key 4-bromocoumarins **37**, **38** [60]. The corresponding

O-linked compounds **39a-d** and **40a-d** were prepared by coupling of intermediates **37** and **38** with various 4-[(2-aminoethoxy)]-substituted phenols **35a-d**. Demethylation was thus carried out on the compounds **39a-d** and **40a-d** to afford the required derivatives **41a-d** and **42a-d**.



Scheme 4. Synthetic routes of **39a-d**, **40a-d**, **41a-d** and **42a-d**. Reagents and conditions: (a) K₂CO₃, dry acetone, MOMCl, rt, 2 h; (b) 5N NaOH solution, ClCH₂CH₂Cl, TBAB, 75 °C, 4 h; (c) RCl or RCl·HCl, K₂CO₃, KI, DMF, 100 °C, 4 h; (d) concentrated HCl, MeOH, rt, 4 h; (e) POBr₃ (1.1 equiv), 1,2-dichlorobenzene, 170 °C, 4 h; (f) arylamines, Cs₂CO₃ (2 equiv), MeCN, 75 °C, 2-3 h; (g) BBr₃, CH₂Cl₂, rt, 12 h.

3.2. Biological evaluation.

3.2.1. ER α binding affinity assay and cell proliferation assay.

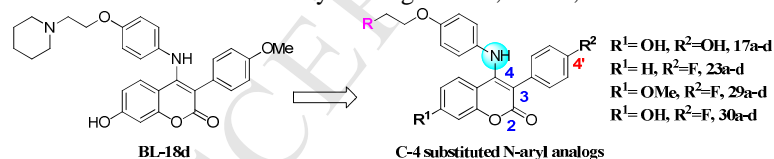
The ER α binding affinities of title molecules were initially measured by following a fluorescence polarization procedure [21, 38 and 39]. Their potency to inhibit the proliferation of human breast cancer cell line MCF-7 (ER+) and human endometrial cancer cell line Ishikawa was also performed using MTT assay. Clearly, the fact that long term treatment of tamoxifen will stimulate endometrial cell growth and increase the incidence of endometrial cancer is a significant concern for its clinical application. Thus, it is essential to evaluate the anti-proliferative activity of new compounds on endometrial cells. For comparison, lead compound **BL-18d**, Tamoxifen and Vandetanib were also used as the positive control in these two assays. These result data can be analyzed in two groups, 4-N-linked analogues and 4-O-linked analogues, and are depicted in Table 1 and Table 2 respectively.

As is shown in Table 1, most of the N-linked compounds (piperidyl substituted as terminal basic group) showed promising binding affinities with IC₅₀ values less than 10 μ M indicating that coumarin scaffold could favorably mimic that of estradiol. It was supposed that hydroxyl group at C-4' position had formed more hydrogen bonds with essential amino acid His524 than methoxyl group in the ligand binding domain of ER α . Expectedly, it is obvious to note that derivatives **17d** with hydroxyl substituted at C-4' position (IC₅₀ = 3.82 μ M) possessed apparently better affinities to ER α than methoxyl

substituted lead compound **BL-18d** ($IC_{50}=6.64 \mu M$). Overall, the more H donor groups (hydroxyl) were incorporated to coumarin skeleton the better binding affinities were observed in the binding assay (**17d** vs. **BL-18d**). Furthermore, replacement of methoxy with F at *p*-position of 3-phenyl substituent resulted in slightly increased binding affinity (**30d** vs. **BL-18d**), which was consistent with our idea of title compound design. The F containing compounds **30a-d** all held the inhibition rate of more than 90% which were very close to that of Tamoxifen. The highest affinity was observed with compound **17d**, exhibiting binding affinity value of $3.82 \mu M$, which is almost twice higher than **BL-18d** ($IC_{50}=6.64 \mu M$).

As a global observation, most of N-linked compounds presented significant anti-proliferative activity on these two cancer cell lines compared to positive control. Moreover, all the piperidine substituted compounds **17d**, **23d**, **29d** and **30d** which showed the best binding affinity in ER α assay within their respective group also demonstrated the best anti-proliferative activity against MCF-7 cells ($IC_{50} = 18.74, 11.32, 12.58$ and $7.06 \mu M$, respectively), which indicated an ER α pathway on the anti-proliferative activity (Table 1). A close observation of the data showed that fluorine containing prototypes (**30a-d**) were more active than their hydroxyl counterpart compounds **17a-d**. Contrary to the trend observed in ER α binding assay, it was interesting to find that an increase in the number of hydroxy groups decreased their anti-proliferative activities, which might be due to their lower cellular uptake. Of all the active compounds, **30d** showed maximum inhibition of cell growth against MCF-7 cells with an IC_{50} of $7.06 \mu M$, about 2 fold more potent than both Tamoxifen ($14.35 \mu M$) and Vandetanib ($16.52 \mu M$), whereas, compound **29d** showed maximum inhibitory effect against Ishikawa cells with an IC_{50} of $8.71 \mu M$.

Table 1
SAR of C-4 substituted N-aryl analogs **17a-d**, **23a-d**, **29a-d** and **30a-d**.



Compound	R ¹	R ²	R	ER α binding affinity ^a		Cytotoxicity (IC_{50} , μM) ^b	
				Inh% at 10 μM	IC_{50} (μM)	MCF-7	Ishikawa
17a	OH	OH		68.46 \pm 5.17	8.21	28.35 \pm 4.35	30.21 \pm 4.24
17b	OH	OH		86.26 \pm 6.07	5.97	27.52 \pm 5.17	29.07 \pm 5.94
17c	OH	OH		83.13 \pm 4.06	6.43	20.65 \pm 3.12	26.69 \pm 4.36
17d	OH	OH		91.61 \pm 7.48	3.82	18.74 \pm 2.84	24.59 \pm 5.27
23a	H	F		34.21 \pm 2.09	ND ^c	32.46 \pm 6.43	28.49 \pm 4.48
23b	H	F		31.76 \pm 2.27	ND	26.38 \pm 3.27	24.65 \pm 2.94
23c	H	F		36.92 \pm 2.27	ND	26.11 \pm 4.63	25.73 \pm 3.67

23d	H	F		76.48 ± 5.15	7.79	11.32 ± 2.25	10.26 ± 1.34
29a	OMe	F		34.97 ± 3.83	ND	31.57 ± 4.74	13.54 ± 1.49
29b	OMe	F		37.34 ± 6.77	ND	26.31 ± 2.66	17.89 ± 2.05
29c	OMe	F		43.29 ± 4.58	ND	21.53 ± 3.15	12.48 ± 2.12
29d	OMe	F		79.52 ± 5.15	7.96	12.58 ± 1.89	8.71 ± 1.53
30a	OH	F		90.38 ± 4.97	6.62	19.29 ± 3.32	24.84 ± 3.17
30b	OH	F		90.88 ± 7.39	4.37	17.46 ± 1.29	17.18 ± 2.78
30c	OH	F		93.67 ± 4.82	4.53	13.94 ± 2.08	21.47 ± 3.09
30d	OH	F		94.94 ± 8.75	3.86	7.06 ± 1.41	10.44 ± 2.62
BL-18d	-	-	-	86.47 ± 5.49	6.64	11.39 ± 3.63	14.38 ± 2.82
Tamoxifen	-	-	-	94.79 ± 9.87	2.67	14.35 ± 3.47	20.65 ± 4.52
Vandetanib	-	-	-	-	-	16.52 ± 2.12	-

^aPercent inhibition of each compound was calculated from the polarization values, shown as mean ± SD of three experiments. The IC₅₀ values are calculated when the Inh% at 10 μM is more than 50%.

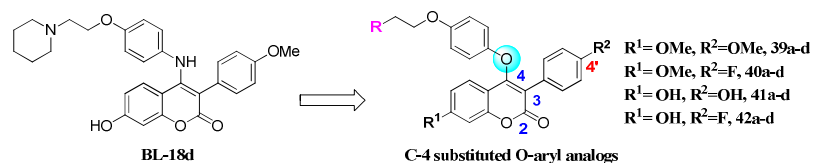
^bThe concentration of compound that inhibit 50% of the cell growth after 48 h of drug exposure measured by MTT assay. Each value was shown as mean ± SD of three experiments.

^cND stands for not determined (IC₅₀ > 10 μM for ERα binding affinity).

On the other hand, overall, the series of O-linked analogues showed a similar trend in both ERα binding affinity assay and cell proliferation assay (Table 2): i) more donor group (hydroxyl) led to higher affinities while their dihydroxy analogs **41a-d** displayed poor cytotoxicity against these two cancer cell lines; ii) among these four basic side substituents, piperidyl (**39d**, **40d**, **41d** and **42d**) was the most optimized group which made great contribution to their ERα binding affinity and anti-proliferative activity. Expectedly, it seemed that introducing of bioisosteric O atom at the C-4 position of coumarin scaffold is beneficial to improve the inhibitory potency, especially in ERα binding affinity assay (**30a-d** vs. **42a-d**). Interestingly, the dimethoxyl compounds **40a-d** which were less potent in ERα binding assay manifested slightly greater potency than the corresponding dihydroxyl compounds **41a-d** against both MCF-7 and Ishikawa cells which also confirmed that the obtained antiproliferative activity might not be only through ERα. What's more, among these O-linked analogues, **40d** was found to exhibit the strongest inhibitory effect against MCF-7 cells (IC₅₀ = 9.32 ± 1.29 μM) and Ishikawa cells (IC₅₀ = 8.41 ± 1.12 μM). Finally, among all the compounds of two series, compound **42d** (R¹=OH, R²=F) were found to be the most potent ERα ligand embodying the highest affinity with IC₅₀ value of 2.19 μM.

Table 2

SAR of C-4 substituted O-aryl analogs **39a-d**, **40a-d**, **41a-d** and **42a-d**.



Compound	R ¹	R ²	R	ERα binding affinity ^a		Cytotoxicity (IC ₅₀ , μM) ^b	
				Inh% at 10 μM	IC ₅₀ (μM)	MCF-7	Ishikawa
39a	OMe	OMe		34.37 ± 5.64	ND ^c	17.84 ± 2.23	11.44 ± 2.55
39b	OMe	OMe		38.93 ± 6.89	ND	15.35 ± 3.69	9.32 ± 1.14
39c	OMe	OMe		34.28 ± 4.58	ND	14.38 ± 2.43	8.53 ± 1.08
39d	OMe	OMe		62.48 ± 4.42	9.42	9.62 ± 1.59	7.47 ± 1.57
40a	OMe	F		72.86 ± 8.52	8.96	15.26 ± 2.38	17.34 ± 2.25
40b	OMe	F		46.83 ± 6.89	ND	16.64 ± 2.35	15.72 ± 1.63
40c	OMe	F		38.32 ± 8.42	ND	14.56 ± 3.64	15.14 ± 1.76
40d	OMe	F		85.79 ± 10.23	6.87	9.32 ± 1.29	8.41 ± 1.12
41a	OH	OH		68.76 ± 3.57	8.43	41.38 ± 6.32	36.97 ± 6.79
41b	OH	OH		46.36 ± 4.84	ND	>50	>50
41c	OH	OH		86.52 ± 7.13	6.84	23.88 ± 3.64	24.53 ± 4.06
41d	OH	OH		92.46 ± 8.12	2.62	19.68 ± 2.55	28.37 ± 3.94
42a	OH	F		84.32 ± 7.47	6.43	16.61 ± 2.94	18.7 ± 2.37
42b	OH	F		93.67 ± 9.38	3.55	21.33 ± 3.62	17.4 ± 1.96
42c	OH	F		91.25 ± 8.53	4.27	16.78 ± 1.59	22.61 ± 4.18
42d	OH	F		95.74 ± 8.45	2.19	9.54 ± 2.65	11.12 ± 2.34
BL-18d	-	-	-	86.47 ± 5.49	6.64	11.39 ± 3.63	14.38 ± 2.82
Tamoxifen	-	-	-	94.79 ± 9.87	2.67	14.35 ± 3.47	20.65 ± 4.52
Vandetanib	-	-	-	-	-	16.52 ± 2.12	-

^aPercent inhibition of each compound was calculated from the polarization values, shown as mean ± SD of three experiments. The IC₅₀ values are calculated when the Inh% at 10 μM is >50%.

^bThe concentration of compound that inhibit 50% of the cell growth after 48 h of drug exposure measured by MTT assay. Each value was shown as mean ± SD of three experiments.

^cND stands for not determined (IC₅₀>10 μM for ERα binding affinity).

Based on the above results, we found that all the piperidine substituted compounds **17d**, **23d**, **29d**, **30d**, **39d**, **40d**, **41d** and **42d** which exhibited the best binding affinity in ERα assay within their respective group also demonstrated potent anti-breast cancer activity against MCF-7, as well as good anti-endometrial hyperplasia activity against Ishikawa cells with IC₅₀ value less than 25 μM. Results presented in Figure 4A indicate that all the tested compounds inhibited cell proliferation in a dose-dependent manner. From Figure 4B it is evident that most of the piperidine containing compounds displayed comparable to higher potency than **BL-18d** and tamoxifen against MCF-7 and Ishikawa

cells.

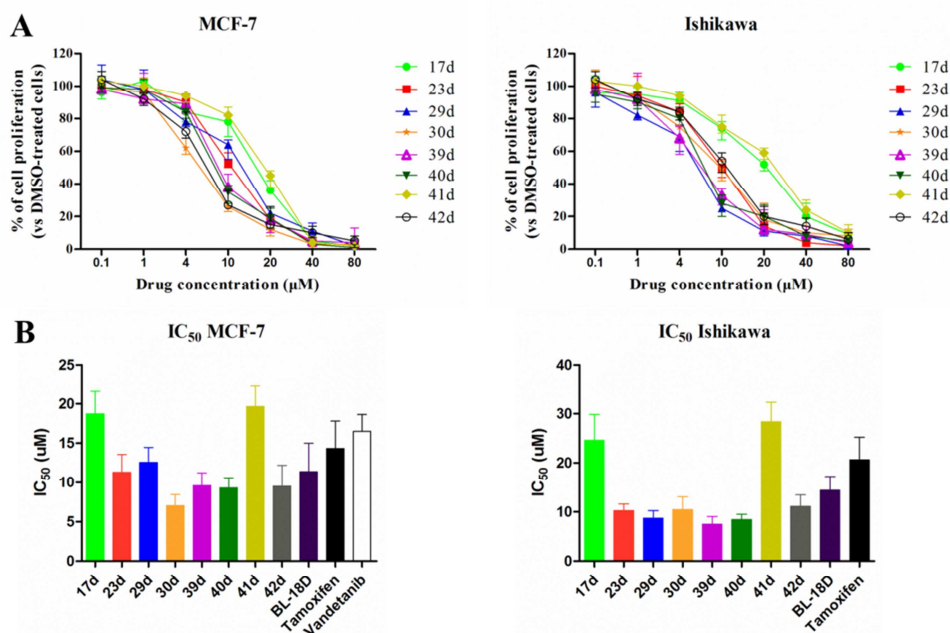


Figure 4. *In vitro* anti-proliferative properties of selected compounds against MCF-7 and Ishikawa cell lines. (A) Growth inhibition assay performed on MCF-7 and Ishikawa cell cells using MTT after 48 h incubation with a range of drug concentrations. Points: % of cell proliferation as compared to untreated control cells, means of at least three individual experiments. (B) Histogram representation of the micromolar concentration of the compounds required to inhibit 50% of MCF-7 and Ishikawa cell proliferation after 48 h drug incubation (IC₅₀). Columns: means of at least three individual experiments; bars: SD.

3.2.2. Antiangiogenic activity evaluation.

On the basis of preliminary ER α binding affinity and cancer cell proliferation activity, several potent compounds were screened *in vitro* for their antiproliferative potency against VEGFR-2 overexpressed human umbilical vein endothelial cells (HUVEC) and VEGFR-2 inhibitory activity with Vandetanib as positive control. As shown in Table 4, most of the tested compounds manifested considerable inhibitory activity on VEGFR-2 compared with Vandetanib. Three compounds **17d**, **30d** and **42d** showed 82.91-88.42% inhibition against VEGFR-2 in contrast to Vandetanib which showed inhibition percentage of 95.73%. Results of HUVEC cell proliferation assay indicated that five of selected compounds (**29d**, **30d**, **39d**, **40d** and **42d**) displayed potent antiproliferative activities with IC₅₀ values ranging from 7.64 to 15.73 μ M. Their potency were comparable with the reference drug Vandetanib but better than **BL-18d** (IC₅₀=16.19 μ M). Particularly, **39d** showed the highest anti-proliferative activity with IC₅₀ values of 7.64 μ M. It is worthy to note that the dihydroxyl

containing compounds **17d** and **41d** only showed fair cell-growth inhibitory effect against HUVEC, which was in accordance with their low potency against MCF-7 and Ishikawa cells.

Table 3

Antiangiogenic activity of representative compounds **17d**, **23d**, **29d**, **30d**, **39d**, **40d**, **41d** and **42d**.

compound	VEGFR-2 Inhibition ^a (%)	HUVEC (IC ₅₀ , μM) ^b
Vandetanib	95.73 ± 2.15	6.76 ± 0.68
BL-18d	59.34 ± 4.64	16.19 ± 2.07
17d	83.25 ± 8.83	30.79 ± 4.52
23d	41.84 ± 3.26	17.15 ± 1.63
29d	66.01 ± 6.71	9.05 ± 1.38
30d	88.42 ± 8.12	9.92 ± .084
39d	67.63 ± 2.05	7.64 ± 0.97
40d	55.13 ± 3.68	13.57 ± 1.01
41d	66.08 ± 6.32	23.94 ± 3.62
42d	82.91 ± 6.43	15.73 ± 1.42

^aPercentage inhibition of each compound on VEGFR-2 at 40 μM was measured using homogeneous time resolved fluorescence (HTRF) assay, shown as mean ± SD of three experiments.

^bThe concentration of compound that inhibit 50% of the cell growth after 48 h of drug exposure measured by MTT assay. Each value was shown as mean ± SD of three experiments.

In summary, we found that compound **42d** exhibited the strongest ER α binding affinity (IC₅₀= 2.19 μM) and excellent cytotoxicity for MCF-7 and Ishikawa cells (IC₅₀ = 9.54 ± 2.65 and 11.12 ± 2.34 μM, respectively), also was a promising anti-angiogenesis agent (82.91% of VEGFR-2 inhibition; IC₅₀= 15.73 μM against HUVEC cells). Thus, **42d** was selected for our further investigation of its multifunctional effects.

3.2.3. Effect of **42d** on migration of MCF-7 cells

Metastasis is the major cause of death of the advanced breast cancer patients. Although many breast cancers respond well to chemotherapy initially, they become aggressive, recur and metastasize once they develop resistance [61]. Cell migration is usually associated with a metastatic phenotype; herein we adopted a wound-healing migration assay to determine the ability of **42d** to inhibit the migration of MCF-7 cells. The results showed that in the absence of **42d**, the cells migrated within 48 h to fill most of scratched area, but the noncytotoxic treatment of **42d** significantly prevented this migration of MCF-7 cells in a dose- and time-dependent manner (Fig. 5).

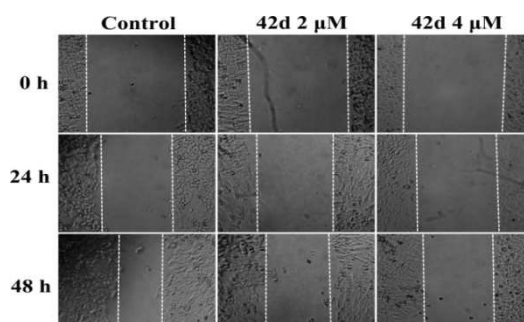


Figure 5. Effects on the migration of MCF-7. Representative images of MCF-7 cells treated with serum-free 1640 medium containing **42d** (2 and 4 μM) for 24 and 48 h were photographed under phase contrast microscopy (magnification, 100 \times). Control was treated with serum-free 1640 medium.

3.2.4. Effect of **42d** on Cell Cycle distribution in human breast cancer MCF-7 cells

In MCF-7 human breast cancer cells, tamoxifen exerts anti-estrogenic effects, marked by slowing of cellular proliferation, with the cells arrested in the G1 phase of the cell cycle [62]. Thus, we further evaluated the effect of **42d** on the distribution of the cells in cell cycle with Tamoxifen as positive control. Representative cell-cycle changes were detected in MCF-7 cells after exposure to DMSO (control), Tamoxifen (2 μM) and **42d** (2 μM , 4 μM and 6 μM) for 24 h (Fig. 6). As is seen from the results, compound **42d** concentration-dependently arrested cell cycle at G0/G1 phase, accompanied with decrease of cells at G2/M and S phase for MCF-7 cells. This indicates that the G0/G1 arrest in MCF-7 cells by compounds **42d** also made contribution to its potent anti-proliferative activity.

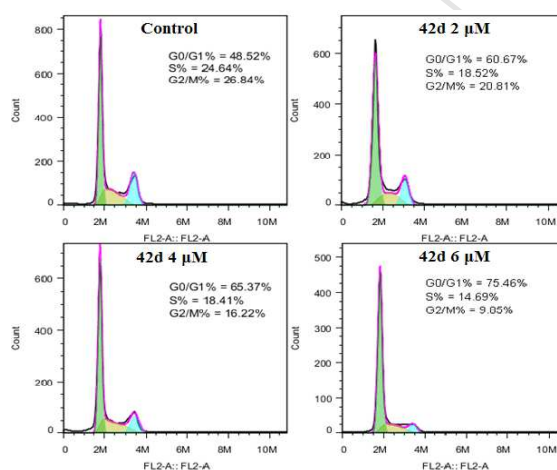


Figure 6. (A) Cell cycle analysis of MCF-7 cells treatment of compound **42d** (2, 4 and 6 μM) and Tamoxifen (2 μM) as positive control for 24 h.

3.2.5. The inhibition activity of compound **42d** against the expression of progesterone receptor microRNA in MCF-7 cells.

To evaluate the transcriptional level of ER α -regulated target genes, we further adapted quantitative real-time polymerase chain reaction (RT-PCR) in the ER positive MCF-7 cells to investigate the expression of progesterone receptor (PgR). The progesterone receptor expression is commonly associated with estrogenic or antiestrogenic activity. As shown in Fig. 7, presence of 10 nM estradiol (E2) was able to remarkably elevate the mRNA expression of PgR gene compared to the vehicle control. Observably, compound **42d** at the concentration of 1 μM in combination with 10 nM E2 dramatically reduced the expression of PgR mRNA induced by E2 (***) P < 0.001 vs. E2 group).

Furthermore, **42d** exhibited stronger antagonism against the expression of PgR mRNA than positive control Tamoxifen at the concentration of 1 μ M in the presence of 10 nM E2, indicating that **42d** presented significantly antiestrogenic property.

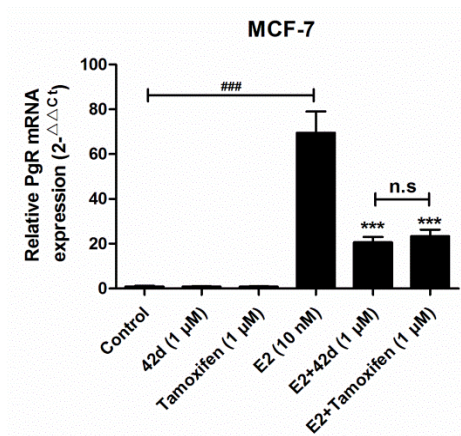


Figure 7. The increased mRNA expression of PR induced by E2 was reversed by **42d** in MCF-7 cells. The mRNA expression of PR was examined by Real-time PCR. Values are mean \pm SD (n=3). * P < 0.05, ** P < 0.01, *** P < 0.001 vs. E2 group. # P < 0.05, ## P < 0.01, ### P < 0.001.

3.2.6. Effect of **42d** on VEGFR-2 phosphorylation

VEGF signalling pathway through the VEGFR-2 tyrosine kinase phosphorylation displays a crucial role in angiogenesis. What's more, VEGFR-2 is expressed at high level in many kinds of cancers [63]. Disruption of VEGF signaling pathway by either specific binding of circulating VEGF or inhibiting receptor tyrosine kinases with small molecules has been found to inhibit angiogenesis, tumor progression and dissemination. To confirm our hypothesis, a Western blotting assay for total and phosphorylated (active) VEGFR-2 was performed. As shown in Fig. 8, **42d** was able to block the phosphorylation of VEGFR-2 in a dose dependent manner. Sunitinib was used as the positive control. At the concentration of 4 μ M, **42d** significantly decreased the active form of VEGFR-2 (Fig. 8B) (***) (p < 0.001 vs. control). Moreover, at concentrations of 2 μ M, compounds **42d** presented a slightly better effect than Sunitinib.

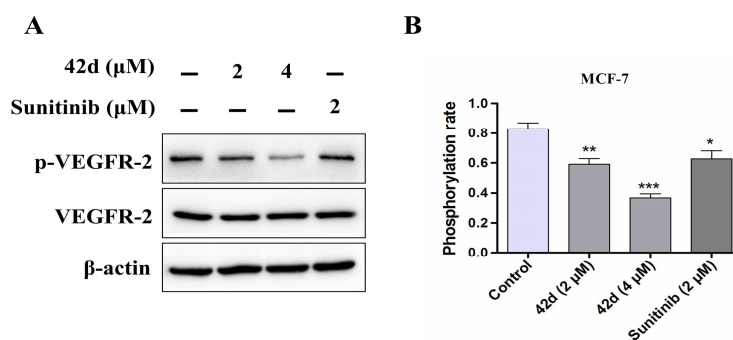


Figure 8. **42d** inhibits the phosphorylation of VEGFR-2 in MCF-7 cells. (A) Expression of p-VEGFR-2 and VEGFR-2 in MCF-7 cells were examined by western blots. (B) Densitometric analysis was performed to determine the phosphorylation rate of VEGFR-2. Values are mean \pm SD (n = 3). *P < 0.05, **P < 0.01, ***P < 0.001 vs. Control group.

3.2.7. **42d** inhibits the MAPK signaling cascade as the result of VEGFR-2 phosphorylation blockade in MCF-7 cells.

Multifactorial pathways have been shown to develop tamoxifen resistance in both preclinical and clinical studies, including the crosstalk between ER and growth factor pathways [64, 65]. The Raf-1/MAPK/ERK pathway is an important cell signaling pathways and controls multiple cellular processes, such as cell proliferation and differentiation [66]. Currently, studies have revealed that over-expression and aberrant activation of Raf-1/MAPK/ERK pathway is associated with the resistance of endocrine therapy [67]. Crosstalk of estrogen receptor pathway with Raf-1/MAPK/ERK pathway is also relative to breast cancer cell migration, invasion, and angiogenesis [68]. Therefore, the blockage of Raf-1/MAPK/ERK pathway is supposed to enhance the effect of anti-hormonal therapy and retard endocrine resistance. Compound **42d** has shown its anti-angiogenesis effect through inhibition on VEGFR-2 activation; we made further investigation of **42d** on inhibiting the downstream Raf-1/MAPK/ERK pathway transduction in MCF-7 cells to explore its underlying mechanism of action. Two effectors, Raf-1 and ERK were examined to study how **42d** affected the Raf-1/MAPK/ERK pathway. As expected, the results indicated that **42d** significantly inhibited p-Raf-1 and p-ERK1/2 activation in a dose-dependent manner, while the total protein level of Raf-1 and ERK1/2 were not altered (Fig. 9).

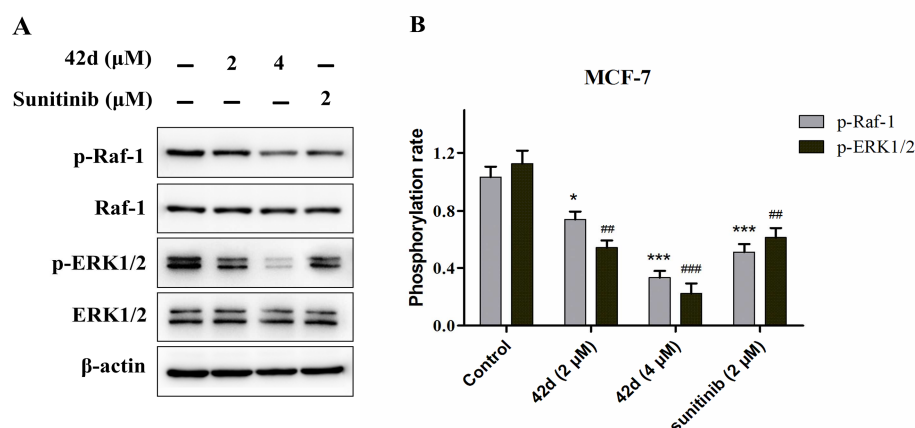


Figure 9. **42d** inhibits the activity of the Raf-1/ERK pathway in MCF-7 cells. (A) Expression of p-Raf-1, Raf-1, p-ERK1/2, and ERK1/2 were examined by western blots in MCF-7 cells. (B) Densitometric analysis was performed to determine the phosphorylation rate of Raf-1 and ERK1/2. Values are mean \pm SD (n = 3). *P < 0.05, **P < 0.01, ***P < 0.001 vs. Control group; #P < 0.05, ##P < 0.01, ###P < 0.001 vs. Control group.

3.2.8. Potential mechanisms of designed compound **42d** on ER α - and VEGFR-2-mediated signaling pathways

Estrogen receptor- α (ER α), a member of the nuclear receptor family, is activated by the endogenous estrogen 17 β -estradiol (E2) to regulate proliferation-dependent gene expression. Our compound **42d** was able to compete with circulating estrogen for binding (ER α), consequently leading to proliferation inhibition and PgR gene down-regulation (Fig. 10). On the other hand, cancer cell proliferation and migration as well as angiogenesis promoted by the crosstalk of estrogen receptor pathway with Raf-1/MAPK/ERK pathway were also restrained by **42d** via the phosphorylation blockade of VEGFR-2, Raf-1 and ERK1/2. This synergistic inhibitory effect of **42d** on ER α and VEGFR-2/Raf-1/MAPK/ERK pathway suggested it a promising multifunctional agent against breast cancer. And this work opens a novel way to the design of multi-targeted agents targeting ER α and VEGFR-2 in the therapy of some breast cancers.

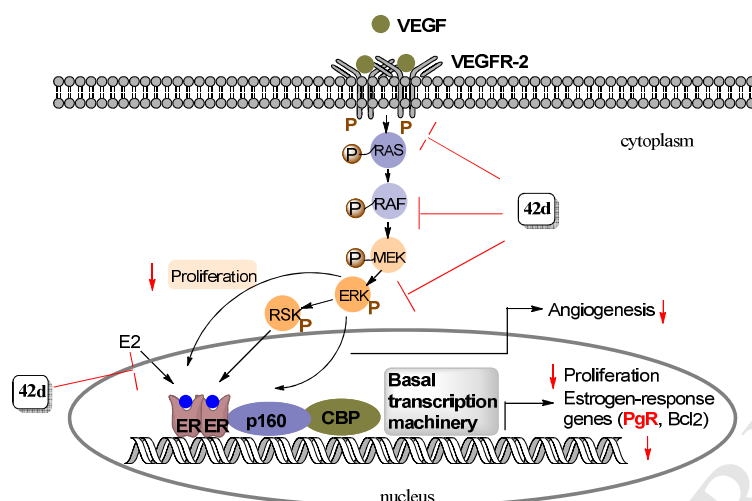


Figure 10. Schematic representation elucidating the role of **42d** in interfering with signaling pathways initiated by ER α and VEGFR-2

3.3. Molecular modeling studies.

The designed inhibitors were subsequently subjected to docking analysis in ER α (PDB ID: 3ERT) and VEGFR-2 (PDB ID: 1YWN) proteins. The docking interaction energies obtained for the designed candidates docked within the active site of both the proteins showed favorable binding modes for all docked compounds, where all ligands had good scores between -49.59 and -69.26 kcal/mol (Table 4). Compound **41d** endowed with two H-bond donor groups (hydroxyl) achieved the lowest docking score amongst all synthesized compounds within both proteins, which was in line with our idea of drug design. Furthermore, the O linked analogues **40d**, **41d** and **42d** exhibited better scores within ER α protein than their N linked counterparts **29d**, **17d** and **30d**, which was in line with the experimental ER α binding affinities indicating a good correlation between predicted binding energies and the corresponding experimental affinities scoring functions. The docking energy scores observed within both ER α and VEGFR-2 proteins are mentioned in the supplementary data.

To further support our structural modifications, a deeper binding mode analysis was performed on the promising compounds **42d**. As depicted in Fig. 11A, the docked pose of **42d** in ER α active site revealed that the core skeleton of 3-aryl-4-aryloxy-2H-chromen-2-one is favorably positioned into the binding site. Furthermore, an excellent superimposition of **42d** over the structure of 4-hydroxytamoxifen (OHT, co-crystallized ligand) was observed. And its basic side chain pointed toward Asp351 to generate an antagonistic conformation as that of 4-OHT. Detailed docking results from Fig. 11B showed that hydroxy group of the coumarin moiety formed hydrogen bonding interaction with Glu353 (2.86 Å) and Arg394 (2.80 Å), while the *p*-methoxy of C-3 substituted benzyl ring interacted with His524 amino acid residue (3.09 Å) and formed an essential hydrogen bond. This indispensable ER α binding mode of **42d** which is the typical character of selective estrogen receptor

modulator contributed greatly to its antiestrogenic property.

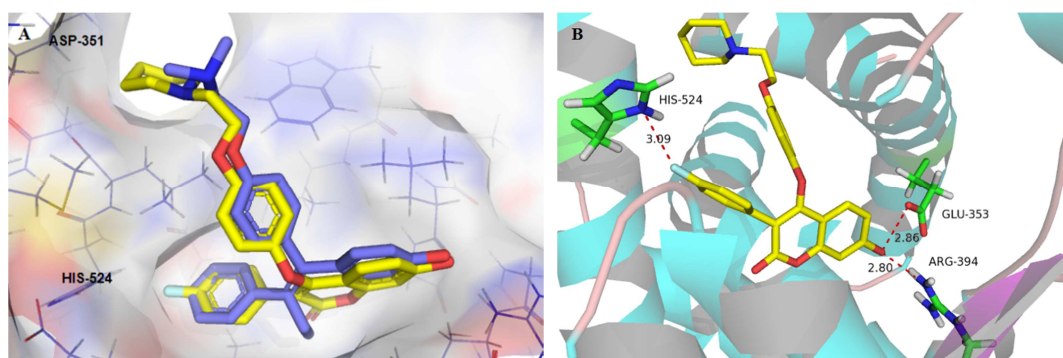


Figure 11. (A) Superimposed poses of OHT (blue) with representative derivatives **42d** (yellow), binding to ER α , the protein was shown in surface. (B) Docking interactions of **42d** within ER α active site (surrounding residues shown as green sticks). Dotted lines (red) represent the hydrogen bonding interaction.

The binding orientation of **42d** within the ligand binding domain of VEGFR-2 showed a binding mode which was different with Sunitinib but similar to that of diaryl urea VEGFR-2 inhibitors [69]. The docking analysis of compound **42d** within VEGFR-2 protein showed hydrogen bonding interaction of hydroxy group of coumarin with an essential amino acid Cys917 (2.68 and 2.92 Å) in the ATP hinge region (Fig. 12). Moreover, the coumarin ring was docked into a hydrophobic pocket, creating a π - π stacking interaction with the aromatic ring of Phe916 (6.12 Å), providing further stabilization for the ligand-receptor complex. The side chain of **42d** pointed toward a hydrophobic region which was commonly occupied by the diaryl urea fragment. These docking results may provide additional insights into the protein-ligand interactions and potential structural modifications for further activity improvement.

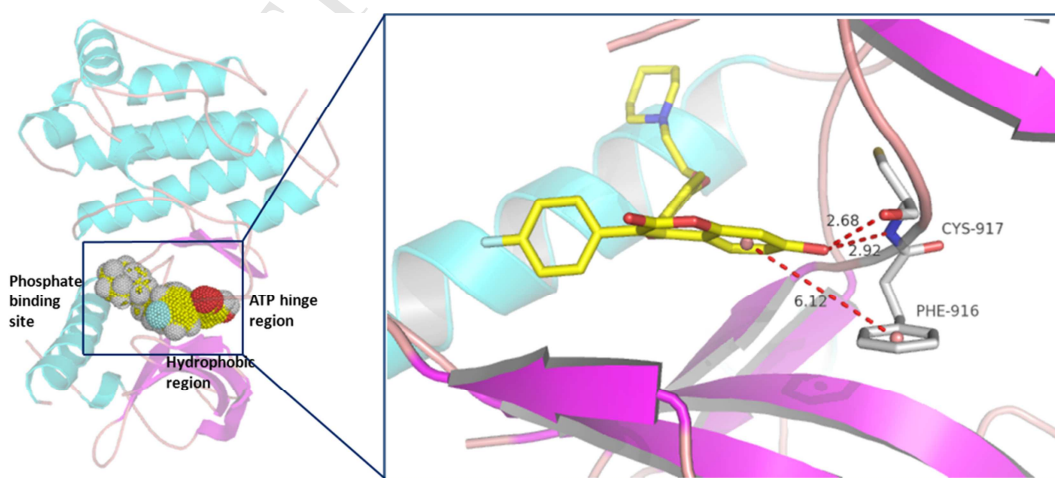


Figure 12. The binding mode of compound **42d** (ball and stick in yellow) docked into the VEGFR-2 binding site (surrounding residues shown as gray sticks). Hydrogen bonding and hydrophobic interactions are shown as red

dotted lines with distances in angstrom.

4. Conclusion

In summary, what described here is the rationally guided optimization of a series of 3-aryl-4-aniline/aryloxy-2H-chromen-2-one derivatives through structure-based modification of lead compound **LE-18d** in order to obtain multifunctional effect towards ER α and VEGFR-2. By means of bioisosteric replacement, O atom was attached to the 4-position of coumarin moiety, while F atom was incorporated to C-4' position of 3-phenyl substituent with the hope of retaining necessary interactions with essential amino acid residues of targeted ER α receptor and VEGFR-2 enzyme. Among them, O linked compounds not only exhibited potent ER α binding affinities, but also showed promising anti-proliferative activities against both cancer cells and angiogenesis-related cells *in vitro*. Further mechanism investigation revealed that **42d** was able to inhibit MCF-7 cell migration and arrest cell cycle at G0/G1 phase in MCF-7 cells in a concentration-dependent manner. In addition to its significant antiestrogenic property observed in RT-PCR, **42d** was also able to inhibit the activation of VEGFR-2 and the signaling transduction of Raf-1/MAPK/ERK pathway in MCF-7 cells. Molecular docking analysis of **42d** indicated this molecule assumed a well-known ER α binding mode embodying three essential hydrogen bonding interactions, which is the typical character of selective estrogen receptor modulator. Additionally, docking interaction within VEGFR-2 revealed that **42d** has the ability to occupy the ATP region of VEGFR-2 enzyme via forming a stronger π - π stacking interaction and two hydrogen bonding interactions with key amino acid residues.

Finally, all these results together open a new avenue for the development of multifunctional agents targeting ER α and VEGFR-2 in the therapy of some breast cancers. Further *in vivo* anticancer effects of promising compound **42d** on 4T1 induced BALB/c mice breast cancer models are in progress and will be reported in due course.

5. Experimental section

5.1 Chemistry

5.1.1. General.

Most chemicals and solvents were of analytical grade and, when necessary, were purified and dried by standard methods. Reactions were monitored by thin-layer chromatography (TLC) using precoated silica gel plates (silica gel GF/UV 254), and spots were visualized under UV light (254 nm). Melting points (uncorrected) were determined on a Mel-TEMP II melting point apparatus and are uncorrected. ^1H NMR and ^{13}C NMR spectra were recorded with a Bruker Avance 300 MHz spectrometer at 300 K, using TMS as an internal standard. MS spectra were recorded on a Shimadzu

GC-MS 2050 (ESI) or an Agilent 1946A-MSD (ESI) Mass Spectrum. Column chromatography was performed with silica gel (200-300 mesh). Chemical shifts (δ) are expressed in parts per million relative to tetramethylsilane, which was used as an internal standard, coupling constants (J) are in hertz (Hz), and the signals are designated as follows: s, singlet; d, doublet; t, triplet; m, multiplet.

Analytical HPLC for assessing purity was performed on Agilent 1260 Infinity System equipped with a UV detector at 254 nm. The column employed is an Agilent Zorbax AB-C18 chromatography column (5 μ m, 4.6 \times 250 mm). Unless otherwise indicated, the purity of the final products was >95% (Supplementary data).

5.1.2. General method I: sulfonic esterification

Compounds **21** or **27** (2 mmol) was dissolved in 10 mL of dry dichloromethane and to it was added dry TEA (0.56 g, 5.60 mmol) and stirred at room temperature until the reaction mixture became homogeneous. The total reaction mixture was then put on an ice bath, 4-toluenesulfonylchloride (0.42 g, 2.2 mmol) was added dropwise stirred for 10 more minutes; the ice bath was removed and the reaction mixture continued to be stirred at room temperature for another 30 min. The solvent was evaporated and the solid purified by column chromatograph to give a white solid **22** or **28**.

5.1.3. General method II: SN2 nucleophilic substitution.

A mixture of compound **14** or **22** or **28** (0.47 mmol), four kind of anilines (1.0 equiv.), and K_2CO_3 (2.0 equiv.) in ethanol (6.0 mL) was stirred at 75 °C for 2-3 h. After completion of the reaction as indicated by TLC, the mixture was cooled to room temperature and then extracted, evaporated and purified directly by flash column chromatography on silica gel to afford the corresponding pure products **16a-d**, **23a-d** and **29a-d**.

5.1.4. General method III: demethylation.

A solution of **16a-d** or **29a-d** or **39a-d** or 40a-d (0.4 mmol) in dry CH_2Cl_2 (10 mL) was cooled to -30 °C by cryotrap. A solution of BBr_3 (2.4 mmol) in dry CH_2Cl_2 (2.4 mL) was added dropwise under nitrogen. The mixture was gently warmed to room temperature and stirred for 12 h. The reaction mixture was quenched with H_2O (50 mL), then saturated sodium bicarbonate solution was adjusted to pH=8. The precipitate was collected by filtration, and further purified by silica gel column chromatography to afford the demethylation product **17a-d**, **30a-d**, **41a-d** and **42a-d**.

5.1.5. Synthesis of intermediates **16a-d**

Intermediates **16a-d** were prepared by our group previously and associated NMR and HR-MS characterization were reported in previous published paper [21].

5.1.6. General synthesis of final compounds **17a-d**

Final compounds **17a-d** were prepared according to *General method III: demethylation*, yield 44.5-61.6%.

5.1.7. *4-((4-(2-(dimethylamino)ethoxy)phenyl)amino)-7-hydroxy-3-(4-hydroxyphenyl)-2H-chromen-2-one (17a)*

Light yellow solid, yield 44.5%, mp 156-158°C; ¹H NMR (300 MHz, DMSO) δ (ppm): 9.33 (s, 1H), 8.12 (s, 1H), 7.67 (d, *J* = 8.8 Hz, 1H), 6.91 (d, *J* = 8.4 Hz, 2H), 6.74 – 6.63 (m, 4H), 6.63 (d, *J* = 8.8 Hz, 2H), 6.52 (d, *J* = 8.4 Hz, 2H), 3.92 (t, *J* = 5.9 Hz, 2H), 3.68 (s, 3H), 2.59 (t, *J* = 5.5 Hz, 2H), 2.23 (s, 6H). ¹³C NMR (75 MHz, DMSO) δ: 162.3, 161.1, 156.4, 154.5, 154.5, 148.2, 134.8, 132.2, 126.4, 125.0, 123.5, 114.8, 114.7, 112.5, 108.9, 103.6, 102.4, 66.4, 57.9, 55.4, 45.8. MS (ESI) *m/z*: 455.1 ([M+Na]⁺). HRMS (ESI) for C₂₅H₂₄N₂O₅+H calcd 432.1720, found 432.1742.

5.1.8. *4-((4-(2-(diethylamino)ethoxy)phenyl)amino)-7-hydroxy-3-(4-hydroxyphenyl)-2H-chromen-2-one (17b)*

Light yellow solid, yield 48.9%, mp 168-171°C; ¹H NMR (300 MHz, DMSO) δ (ppm): 9.32 (s, 1H), 8.11 (s, 1H), 7.69 (d, *J* = 9.0 Hz, 1H), 6.93 (d, *J* = 8.5 Hz, 2H), 6.78 – 6.67 (m, 4H), 6.62 (d, *J* = 8.9 Hz, 2H), 6.53 (d, *J* = 8.5 Hz, 2H), 3.94 (t, *J* = 5.9 Hz, 2H), 2.82 (s, 2H), 2.64 (d, *J* = 6.7 Hz, 4H), 1.01 (t, *J* = 7.1 Hz, 6H). ¹³C NMR (75 MHz, DMSO) δ: 162.4, 160.8, 156.3, 154.5, 154.5, 148.2, 134.9, 132.2, 126.3, 125.0, 123.5, 114.8, 114.7, 112.5, 109.1, 103.7, 102.5, 66.4, 51.5, 47.5, 11.8. MS (ESI) *m/z*: 483.1 ([M+Na]⁺). HRMS (ESI) for C₂₇H₂₈N₂O₅+H calcd 461.2071, found 461.2071.

5.1.9. *7-hydroxy-3-(4-hydroxyphenyl)-4-((4-(2-(pyrrolidin-1-yl)ethoxy)phenyl)amino)-2H-chromen-2-one (17c)*

Light yellow solid, yield 53.2%, mp 134-138 °C; ¹H (300 MHz, DMSO) δ (ppm): 9.34 (s, 1H), 8.20 (s, 1H), 7.72 (d, *J* = 9.3 Hz, 1H), 6.93 (d, *J* = 8.5 Hz, 2H), 6.65 (t, *J* = 6.3 Hz, 4H), 6.65 (d, *J* = 8.5 Hz, 2H), 6.56 (d, *J* = 8.9 Hz, 2H), 3.92 (t, *J* = 5.6 Hz, 2H), 2.75 (t, *J* = 5.7 Hz, 2H), 2.53 (d, *J* = 1.8 Hz, 4H), 1.67 (s, 4H). ¹³C NMR (75 MHz, DMSO) δ: 162.2, 160.7, 157.8, 154.5, 154.3, 147.6, 134.0, 131.5, 126.7, 125.6, 123.6, 113.9, 112.7, 112.0, 108.5, 102.1, 101.7, 66.6, 54.0, 53.8, 23.0. MS (ESI) *m/z*: 481.1 ([M+Na]⁺). HRMS (ESI) for C₂₇H₂₆N₂O₅+H calcd 459.1854, found 459.1862.

5.1.10. *7-hydroxy-3-(4-hydroxyphenyl)-4-((4-(2-(piperidin-1-yl)ethoxy)phenyl)amino)-2H-chromen-2-one (17d)*

Light yellow solid, yield 61.6%, mp 241-243°C; ¹H NMR (300 MHz, DMSO) δ (ppm): 9.47 (s, 1H), 8.04 (s, 1H), 7.66 (d, *J* = 8.6 Hz, 1H), 6.92 (d, *J* = 8.5 Hz, 2H), 6.76 – 6.64 (m, 4H), 6.60 (d, *J* = 8.9 Hz, 2H), 6.52 (d, *J* = 8.5 Hz, 2H), 3.92 (t, *J* = 6.0 Hz, 2H), 2.58 (t, *J* = 5.9 Hz, 2H), 2.47 – 2.35 (m, 4H), 1.57 – 1.45 (m, 4H), 1.37 (d, *J* = 4.9 Hz, 2H). ¹³C NMR (75 MHz, DMSO) δ: 162.4, 160.8, 156.3, 154.5, 154.5, 148.2, 134.93, 132.2, 126.3, 125.0, 123.5, 114.8, 114.7, 112.5, 109.1, 103.6, 102.5, 66.4, 51.5, 47.5, 11.8. MS (ESI) *m/z*: 495.1 ([M+Na]⁺). HRMS (ESI) for C₂₈H₂₈N₂O₅+H calcd 473.2071, found 473.2075.

5.1.11. *4-flourinephenylacetic acid, 2-(methoxycarbonyl)phenyl ester (20)*

To a mixture of methyl salicylate (1.52 g, 10 mmol) and 4-flourinephenylacetic acid (11 mmol) in 10 mL of pyridine at 0-10 °C was added dropwise POCl₃ (1.1 mL, 12 mmol) within 0.5 h under stirring. After the above mixture was stirred for 2 h at 0-10 °C, the concentrated HCl was added to adjust pH 5-6 at the same temperature. The mixture was filtered and washed with water to obtain the crude product with a yield >80%, mp 73-77°C. MS (ESI) m/z: 289.1 ([M+H]⁺).

5.1.12. 3-(4-flourinephenyl)-4-hydroxy-2H-chromen-2-one (21)

The 4-flourinephenylacetic ester of methyl salicylate (5 mmol) was mixed with anhydrous pyridine (10 mL), followed by the addition of KOH powder (0.7 g, 12.5 mmol) at room temperature. After the mixture was stirred for 4 h in a nitrogen atmosphere, 1N HCl was added to adjust pH 3-4. The mixture was filtered and washed with water to obtain the crude product with a yield >45%, mp 234-237°C. MS (ESI) m/z: 255.1 ([M-H]⁻).

5.1.13. 2-Oxo-3-(4-methoxyphenyl)-2H-chromen-4-yl-4-flourinebenzenesulfonate (22)

Intermediate **22** was prepared according to *General method I: sulfonic esterification* as a white solid, yield 77.8%, mp 176-179°C. ¹H (300 MHz, CDCl₃) δ (ppm): 8.23 (d, *J* = 15.5 Hz, 1H), 7.68 (m, 1H), 7.41 (m, 2H), 7.42 (d, *J* = 8.6 Hz, 2H), 7.16 (d, *J* = 8.6 Hz, 2H), 7.07 (d, *J* = 8.2 Hz, 2H), 6.68 (d, *J* = 8.2 Hz, 2H), 2.41 (s, 3H). MS (ESI) m/z: 433.1 ([M+Na]⁺).

5.1.14. General synthesis of final compounds 23a-d

Final compounds **23a-d** were prepared according to *General method II: SN2 nucleophilic substitution*, yield 49.6-64.3%.

5.1.15. 4-((4-(2-(dimethylamino)ethoxy)phenyl)amino)-3-(4-fluorophenyl)-2H-chromen-2-one (23a)

Yellow solid, yield 64.3%, mp 155-156°C; ¹H NMR (300 MHz, DMSO) δ (ppm): 8.60 (s, 1H), 8.06 (d, *J* = 7.8 Hz, 1H), 7.55 (d, *J* = 7.3 Hz, 1H), 7.31 (dd, *J* = 13.3, 8.0 Hz, 2H), 7.01 (dd, *J* = 8.5, 5.7 Hz, 2H), 6.77 (t, *J* = 8.9 Hz, 2H), 6.64 (d, *J* = 8.8 Hz, 2H), 6.49 (d, *J* = 8.8 Hz, 2H), 3.84 (t, *J* = 5.7 Hz, 2H), 2.52 – 2.46 (m, 2H), 2.13 (s, 6H). ¹³C NMR (75 MHz, DMSO) δ: 162.8, 162.11, 159.5, 155.0, 152.7, 148.0, 133.6, 133.4, 133.3, 132.2, 131.1, 124.8, 124.4, 124.0, 117.2, 114.6, 114.4, 114.1, 102.7, 66.5, 57.9, 45.9. MS (ESI) m/z: 419.1 ([M+H]⁺). HRMS (ESI) for C₂₅H₂₃FN₂O₃+H calcd 419.1765, found 419.1766.

5.1.16. 4-((4-(2-(diethylamino)ethoxy)phenyl)amino)-3-(4-fluorophenyl)-2H-chromen-2-one (23b)

Yellow solid, yield 62.4%, mp 138-141°C; ¹H NMR (300 MHz, DMSO) δ (ppm): 8.58 (s, 1H), 8.04 (d, *J* = 7.9 Hz, 1H), 7.54 (t, *J* = 7.6 Hz, 1H), 7.36 – 7.20 (m, 2H), 7.00 (dd, *J* = 8.5, 5.8 Hz, 2H), 6.75 (t, *J* = 8.9 Hz, 2H), 6.63 (d, *J* = 8.8 Hz, 2H), 6.46 (d, *J* = 8.8 Hz, 2H), 3.80 (t, *J* = 6.0 Hz, 2H), 2.63 (t, *J* = 6.0 Hz, 2H), 2.46 – 2.40 (m, 4H), 0.89 (t, *J* = 7.1 Hz, 7H). ¹³C NMR (75 MHz, DMSO) δ: 162.8,

162.1, 159.5, 155.1, 152.7, 148.0, 133.6, 133.4, 133.3, 132.1, 131.2, 124.8, 124.4, 123.9, 117.14, 114.6, 114.4, 114.1, 102.7, 66.9, 51.7, 47.5, 12.2. MS (ESI) m/z : 469.1 ($[M+H]^+$). HRMS (ESI) for $C_{27}H_{27}FN_2O_3+H$ calcd 447.2078, found 447.2085.

5.1.17. *3-(4-fluorophenyl)-4-((4-(2-(pyrrolidin-1-yl)ethoxy)phenyl)amino)-2H-chromen-2-one* (**23c**)

Yellow solid, yield 58.7%, mp 155-157°C; 1H NMR (300 MHz, $CDCl_3$) δ 7.42 – 7.33 (m, 1H), 7.32 – 7.17 (m, 4H), 6.97 (ddd, $J = 15.3, 12.8, 5.0$ Hz, 3H), 6.80 (d, $J = 8.8$ Hz, 2H), 6.72 (d, $J = 8.9$ Hz, 2H), 3.98 (t, $J = 5.9$ Hz, 2H), 2.81 (t, $J = 5.9$ Hz, 2H), 2.54 (s, 4H), 1.72 (d, $J = 3.4$ Hz, 4H). ^{13}C NMR (75 MHz, DMSO) δ 162.3, 161.6, 159.0, 154.6, 152.2, 147.5, 133.0, 132.9, 132.8, 131.7, 130.6, 124.3, 123.9, 123.5, 116.7, 114.1, 113.9, 113.6, 102.2, 66.9, 54.1, 53.9, 23.1. MS (ESI) m/z : 467.1 ($[M+Na]^+$). HRMS (ESI) for $C_{27}H_{25}FN_2O_3+H$ calcd 445.1922, found 445.1921.

5.1.18. *3-(4-fluorophenyl)-4-((4-(2-(piperidin-1-yl)ethoxy)phenyl)amino)-2H-chromen-2-one* (**23d**)

Yellow solid, yield 49.6%, mp 157-159°C; 1H NMR (300 MHz, DMSO) δ (ppm): 8.70 (s, 1H), 8.14 (d, $J = 8.0$ Hz, 1H), 7.67 – 7.60 (m, 1H), 7.41 (dd, $J = 8.3, 1.0$ Hz, 1H), 7.38 – 7.32 (m, 1H), 7.12 – 7.06 (m, 2H), 6.87 – 6.80 (m, 2H), 6.73 – 6.68 (m, 2H), 6.59 – 6.52 (m, 2H), 3.92 (t, $J = 5.9$ Hz, 2H), 2.56 (t, $J = 5.9$ Hz, 2H), 2.45 – 2.35 (m, 4H), 1.49 (dd, $J = 10.9, 5.5$ Hz, 4H), 1.41 – 1.35 (m, 2H). ^{13}C NMR (75 MHz, DMSO) δ : 162.4, 162.1, 159.9, 155.0, 152.7, 148.0, 133.5, 133.4, 133.3, 132.1, 131.1, 124.7, 124.4, 124.0, 117.2, 114.6, 114.4, 114.2, 102.7, 66.4, 57.6, 54.8, 26.1, 24.4. MS (ESI) m/z : 481.1 ($[M+Na]^+$). HRMS (ESI) for $C_{28}H_{27}FN_2O_3+H$ calcd 459.2078, found 459.2086.

5.1.19. *1-(2,4-dihydroxyphenyl)-2-(4-fluorophenyl)ethanone* (**25**)

A mixture of resorcinol (6.67 g, 60.3 mmol) and an appropriate 4-fluorophenylacetic (60.3 mmol) in $BF_3 \cdot OEt_2$ (150 mL) was heated at 85°C for 2.5 hours. The reaction mixture was poured into ice-cold water (300 mL) and extracted with EtOAc twice. The combined organic layer was washed with saturated sodium bicarbonate solution ($NaHCO_3$) and then brine, dried over magnesium sulfate (Na_2SO_4), and concentrated under reduced pressure. The resulting compound was further purified by recrystallization (EtOH and PE). Yellow crystals; yield: 79.8%, mp 143-146°C; 1H (300 MHz, DMSO) δ (ppm): 11.64 (s, 1H), 9.26 (s, 1H), 6.18-7.84 (m, 7H), 4.33 (s, 2H). MS (ESI) m/z : 245.1 ($[M-H]^-$).

5.1.20. *2-(4-fluorophenyl)-1-(2-hydroxy-4-methoxyphenyl)ethanone* (**26**)

At 0 °C, to a solution of compound **25** (15.5 mmol) and MeOH (15.5 mmol) in dry THF (60 mL) were added PPh_3 (15.5 mmol) and DIAD (15.5 mmol) and the mixture warmed to room temperature over 0.5 h. The solution was diluted with EtOAc (150 mL), washed twice with water and brine dried over Na_2SO_4 and concentrated under reduced pressure. Finally, the crude product was purified by column chromatography. White solid; yield: 84.6%, MS (ESI) m/z : 249.1 ($[M-H]^-$).

5.1.21. 3-(4-fluorophenyl)-4-hydroxy-7-methoxy-2H-chromen-2-one (27)

Intermediate **26** (10.29 mmol) was dissolved in 40 ml of diethyl carbonate and was added 2.4 g NaH (102.9 mmol) under an ice bath with vigorous stirring. The temperature was slowly lifted and then stirred at 120 °C for 2 hours under nitrogen atmosphere. After the completion of the reaction, the solvent was evaporated at reduced pressure and the remaining solid was poured on crushed ice. The pH was adjusted to 3 by adding 6 N of hydrochloric acid. The precipitate was collected and purified by column chromatography. White solid; 69.7%, MS (ESI) m/z: 285.1 ([M-H]⁻).

5.1.22. 3-(4-fluorophenyl)-7-methoxy-2-oxo-2H-chromen-4-yl 4-methylbenzenesulfonate (28)

Intermediate **28** was prepared according to General method I: sulfonic esterification as a yellow solid, yield 86.4%, mp 212-215°C. ¹H (300 MHz, CDCl₃) δ (ppm): 7.86 (d, *J* = 9.0 Hz, 1H), 7.26-7.18 (m, 2H), 7.08 (d, *J* = 9.0 Hz, 2H), 6.95 (d, *J* = 8.2 Hz, 2H), 6.90 (dd, *J* = 8.8, 2.4 Hz, 1H), 6.89 (d, *J* = 2.4 Hz, 1H), 6.57 (d, *J* = 8.8 Hz, 2H), 3.83 (s, 3H), 2.42 (s, 3H). MS (ESI) m/z: 441.1 ([M+H]⁺). MS (ESI) m/z: 463.1 ([M+Na]⁺).

5.1.23. General synthesis of final compounds 29a-d

Final compounds **29a-d** were prepared according to *General method II: SN2 nucleophilic substitution*, yield 48.9-63.2%.

5.1.24. 4-((4-(2-(dimethylamino)ethoxy)phenyl)amino)-3-(4-fluorophenyl)-7-methoxy-2H-chromen-2-one (29a)

Yellow solid, yield 63.2%, mp 146-148 °C; ¹H (300 MHz, DMSO) δ (ppm): 8.48 (s, 1H), 7.91 (d, *J* = 8.9 Hz, 1H), 7.04 – 6.94 (m, 2H), 6.91 – 6.82 (m, 2H), 6.74 (t, *J* = 8.8 Hz, 2H), 6.61 (d, *J* = 8.7 Hz, 2H), 6.47 (d, *J* = 8.7 Hz, 2H), 3.84 – 3.75 (m, 5H), 2.45 (t, *J* = 5.7 Hz, 2H), 2.11 (s, 6H). ¹³C NMR (75 MHz, DMSO) δ: 162.7, 162.5, 162.4, 159.5, 155.0, 154.5, 148.5, 133.7, 133.4, 133.3, 131.3, 125.7, 124.7, 114.6, 114.4, 114.1, 111.8, 110.2, 101.1, 100.7, 66.5, 57.9, 56.3, 45.9. MS (ESI) m/z: 471.1 ([M+Na]⁺). HRMS (ESI) for C₂₆H₂₅FN₂O₄+H calcd 449.1871, found 449.1880.

5.1.25. 4-((4-(2-(diethylamino)ethoxy)phenyl)amino)-3-(4-fluorophenyl)-7-methoxy-2H-chromen-2-one (29b)

Yellow solid, yield 58.7%, mp 145-147°C; ¹H (300 MHz, DMSO) δ (ppm): 8.47 (s, 1H), 7.91 (d, *J* = 8.9 Hz, 1H), 7.03 – 6.95 (m, 2H), 6.85 (dd, *J* = 12.5, 3.3 Hz, 2H), 6.74 (t, *J* = 8.7 Hz, 2H), 6.61 (d, *J* = 8.5 Hz, 2H), 6.47 (d, *J* = 8.6 Hz, 2H), 3.80 (d, *J* = 6.2 Hz, 5H), 2.61 (t, *J* = 5.9 Hz, 2H), 2.49 – 2.42 (m, 4H), 0.88 (t, *J* = 7.0 Hz, 6H). ¹³C NMR (75 MHz, DMSO) δ: 162.7, 162.5, 162.3, 159.5, 155.1, 154.5, 148.5, 133.7, 133.4, 133.3, 131.3, 125.7, 124.7, 114.6, 114.4, 114.1, 111.8, 110.2, 101.1, 100.7, 67.1, 56.3, 51.7, 47.5, 12.3. MS (ESI) m/z: 499.1 ([M+Na]⁺). HRMS (ESI) for C₂₈H₂₉FN₂O₄+H calcd 477.2193, found 477.2184.

5.1.26. 3-(4-fluorophenyl)-7-methoxy-4-((4-(2-(pyrrolidin-1-yl)ethoxy)phenyl)amino)-2H-chrom

en-2-one (29c)

Yellow solid, yield 48.9%, mp 129-131°C; ¹H (300 MHz, DMSO) δ (ppm): 8.50 (s, 1H), 7.95 (d, *J* = 8.9 Hz, 1H), 7.08 – 7.01 (m, 2H), 6.97 – 6.88 (m, 2H), 6.81 (t, *J* = 8.8 Hz, 2H), 6.67 (d, *J* = 8.7 Hz, 2H), 6.53 (d, *J* = 8.9 Hz, 2H), 3.88 (dd, *J* = 13.2, 7.4 Hz, 5H), 2.83 (t, *J* = 5.7 Hz, 2H), 2.54 (s, 4H), 1.74 (d, *J* = 3.4 Hz, 4H). ¹³C NMR (75 MHz, DMSO) δ: 162.5, 162.3, 159.5, 154.9, 154.5, 148.5, 133.8, 133.4, 133.3, 131.3, 125.7, 124.7, 114.7, 114.4, 114.1, 111.8, 110.2, 101.1, 100.8, 66.4, 55.8, 54.3, 23.1. MS (ESI) *m/z*: 497.1 ([M+Na]⁺). HRMS (ESI) for C₂₈H₂₇FN₂O₄+H calcd 475.2033, found 475.2028.

5.1.27. *3-(4-fluorophenyl)-7-methoxy-4-((4-(2-(piperidin-1-yl)ethoxy)phenyl)amino)-2H-chromen-2-one (29d)*

Yellow solid, yield 52.7%, mp 133-135°C; ¹H (300 MHz, DMSO) δ (ppm): 8.46 (s, 1H), 7.90 (d, *J* = 8.9 Hz, 1H), 6.99 (dd, *J* = 8.3, 5.8 Hz, 2H), 6.89 – 6.81 (m, 2H), 6.74 (t, *J* = 8.8 Hz, 2H), 6.61 (d, *J* = 8.7 Hz, 2H), 6.47 (d, *J* = 8.8 Hz, 2H), 3.81 (dd, *J* = 12.5, 6.6 Hz, 5H), 2.47 (t, *J* = 5.8 Hz, 2H), 2.30 (s, 4H), 1.40 (s, 4H), 1.29 (d, *J* = 4.9 Hz, 2H). ¹³C NMR (75 MHz, DMSO) δ: 162.7, 162.5, 162.35, 159.5, 155.0, 154.5, 148.5, 133.7, 133.4, 133.3, 131.3, 125.7, 124.7, 114.7, 114.4, 114.1, 111.8, 110.2, 101.1, 100.8, 66.4, 57.6, 56.3, 54.80, 26.1, 24.4. MS (ESI) *m/z*: 511.1 ([M+Na]⁺). HRMS (ESI) for C₂₉H₂₉FN₂O₄+H calcd 489.2184, found 489.2188.

5.1.28. *General synthesis of final compounds 30a-d*

Final compounds **30a-d** were prepared according to *General method III: demethylation*, yield 48.6-60.5%.

5.1.29. *4-((4-(2-(dimethylamino)ethoxy)phenyl)amino)-3-(4-fluorophenyl)-7-hydroxy-2H-chromen-2-one (30a)*

White solid, yield 48.6%, mp 189-191°C; ¹H (300 MHz, DMSO) δ (ppm): 8.45 (s, 1H), 7.87 (d, *J* = 8.8 Hz, 1H), 7.07 – 6.99 (m, 2H), 6.80 (t, *J* = 8.9 Hz, 2H), 6.74 – 6.63 (m, 4H), 6.52 (d, *J* = 8.8 Hz, 2H), 3.88 (t, *J* = 5.8 Hz, 2H), 2.52 (d, *J* = 5.8 Hz, 2H), 2.18 (s, 6H). ¹³C NMR (75 MHz, DMSO) δ: 162.5, 162.2, 161.2, 159.8, 154.86, 154.5, 148.7, 133.9, 133.4, 133.3, 131.4, 125.9, 124.6, 114.7, 114.4, 114.1, 112.7, 108.9, 102.6, 100.3, 66.4, 57.9, 45.8. MS (ESI) *m/z*: 457.2 ([M+Na]⁺). HRMS (ESI) for C₂₅H₂₃FN₂O₄+H calcd 435.1715, found 435.1719.

5.1.30. *4-((4-(2-(diethylamino)ethoxy)phenyl)amino)-3-(4-fluorophenyl)-7-hydroxy-2H-chromen-2-one (30b)*

Yellow solid, yield 52.8%, mp 168-170°C; ¹H (300 MHz, DMSO) δ (ppm): 8.43 (s, 1H), 7.84 (d, *J* = 8.8 Hz, 1H), 7.05 – 6.95 (m, 2H), 6.75 (t, *J* = 8.9 Hz, 2H), 6.69 – 6.59 (m, 4H), 6.48 (d, *J* = 8.6 Hz, 2H), 3.82 (d, *J* = 5.3 Hz, 2H), 2.68 (s, 2H), 2.51 (d, *J* = 7.0 Hz, 4H), 0.91 (t, *J* = 7.0 Hz, 6H). ¹³C NMR (75 MHz, DMSO) δ: 162.4, 161.2, 159.4, 154.9, 154.5, 148.7, 133.9, 133.4, 133.3, 131.4, 125.9, 124.5, 114.6, 114.4, 114.1, 112.7, 108.9, 102.6, 100.3, 66.7, 51.6, 47.5, 12.1. MS (ESI) *m/z*: 485.1 ([M+Na]⁺).

HRMS (ESI) for $C_{27}H_{27}FN_2O_4+H$ calcd 463.2028, found 463.2036.

5.1.31. *3-(4-fluorophenyl)-7-hydroxy-4-((4-(2-(pyrrolidin-1-yl)ethoxy)phenyl)amino)-2H-chromen-2-one (30c)*

Yellow solid, yield 54.2%, mp 214-216°C; 1H (300 MHz, DMSO) δ (ppm): 8.42 (s, 1H), 7.84 (d, $J = 8.7$ Hz, 1H), 7.07 – 6.94 (m, 2H), 6.75 (t, $J = 8.9$ Hz, 2H), 6.69 – 6.58 (m, 4H), 6.49 (d, $J = 8.6$ Hz, 2H), 3.88 (t, $J = 5.5$ Hz, 2H), 2.71 (d, $J = 5.5$ Hz, 2H), 2.50 (s, 4H), 1.63 (s, 4H). ^{13}C NMR (75 MHz, DMSO) δ : 162.6, 162.5, 161.3, 159.4, 154.8, 154.5, 148.7, 133.9, 133.4, 133.3, 131.4, 125.9, 124.5, 114.6, 114.4, 114.1, 112.7, 108.9, 102.6, 100.4, 67.1, 54.4, 54.4, 23.6. MS (ESI) m/z : 483.1 ($[M+Na]^+$). HRMS (ESI) for $C_{27}H_{25}FN_2O_4+H$ calcd 461.1871, found 461.1876.

5.1.32. *3-(4-fluorophenyl)-7-hydroxy-4-((4-(2-(piperidin-1-yl)ethoxy)phenyl)amino)-2H-chromen-2-one (30d)*

Yellow solid, yield 60.5%, mp 103-105°C; 1H (300 MHz, DMSO) δ (ppm): 8.50 (s, 1H), 7.92 (d, $J = 8.8$ Hz, 1H), 7.09 (dd, $J = 8.7, 5.7$ Hz, 2H), 6.85 (t, $J = 9.0$ Hz, 2H), 6.78 – 6.69 (m, 4H), 6.58 (d, $J = 8.9$ Hz, 2H), 3.96 (t, $J = 5.8$ Hz, 2H), 2.67 (d, $J = 5.4$ Hz, 2H), 2.52 (dd, $J = 5.7, 3.9$ Hz, 4H), 1.53 (d, $J = 4.5$ Hz, 4H), 1.42 (d, $J = 4.7$ Hz, 2H). ^{13}C NMR (75 MHz, DMSO) δ : 162.6, 162.4, 161.2, 159.4, 154.8, 154.5, 148.7, 133.9, 133.4, 133.3, 131.4, 125.9, 124.5, 114.7, 114.4, 114.1, 112.6, 108.9, 102.6, 100.4, 66.1, 57.4, 54.6, 25.7, 24.1. MS (ESI) m/z : 497.1 ($[M+Na]^+$). HRMS (ESI) for $C_{28}H_{27}FN_2O_4+H$ calcd 475.2028, found 475.2037.

5.1.33. *4-(methoxymethoxy)phenol (32)*

Chloromethyl methyl ether (30.4 ml, 0.4 mol) was added dropwise to a suspension of hydroquinone (11 g, 0.1 mol) and anhydrous K_2CO_3 (55.2 g, 0.4 mol) in dry acetone (200 ml). The mixture was stirred at room temperature for 2 h. The reaction mixture was then filtrated to remove unreacted base, and the resulting filtrate was evaporated and purified by column chromatography to give the corresponding derivative **32** (11.5 g, 74.7%), brown oil; MS (ESI) m/z : 155.1 ($[M+H]^+$).

5.1.34. *1-(2-chloroethoxy)-4-(methoxymethoxy)benzene (33)*

Under nitrogen atmosphere, a solution of compound **32** (11.5 g, 74.7 mmol), 149 ml sodium hydroxide solution (5 mmol/L), 115 ml 1, 2-dichloroethane and TBAB (2.4 g, 7.47 mmol) was stirred at 75 °C for 4 h. After the completion of the reaction, the solution was diluted with H_2O ; the organic layer was collected and concentrated under reduced pressure to give compound **33** (11.0 g, 68.4%), brown oil; MS (ESI) m/z : 217.1 ($[M+H]^+$).

5.1.35. *General procedure for compounds 34a-d*

Various tertiary amines or their hydrochloride **a-d** (20.8 mmol) was added to a suspension of compound **33** (1.5 g, 6.9 mmol), catalytic amount of KI and anhydrous K_2CO_3 (4.78 g, 34.6 mmol) in DMF (20 ml). The mixture was stirred under nitrogen atmosphere at 100 °C for 4 h. After cooling to

room temperature, EtOAc and H₂O were poured into the reaction mixture. The aqueous layer was extracted with EtOAc. The combined organic layers were washed with water and dried, concentrated in vacuo to afford the products **34a-d**.

5.1.36. General procedure for compounds **35a-d**

Concentrated hydrochloric acid (1.65 ml, 19.6 mmol) was added dropwise to a suspension of **34a-d** (4.89 mmol) in MeOH (15 ml). The mixture was stirred at room temperature for 4 h. The reaction mixture was then concentrated to afford crude products which were further purified by recrystallization from ethanol to give compounds **35a-d** respectively. **35a** (0.45 g, 42.4%), MS (ESI) *m/z*: 182.1[M+H]⁺; **35b** (0.40 g, 32.0%), MS (ESI) *m/z*: 210.1[M+H]⁺; **35c** (0.5 g, 34.4%), MS (ESI) *m/z*: 208.1[M+H]⁺; **35d** (0.6 g, 44.2%), MS (ESI) *m/z*: 222.1[M+H]⁺.

5.1.37. General procedure for compounds **35a-d**

Compound **36** or **27** (40 mmol) and POBr₃ (4.5 mL, 44 mmol) in 1, 2-dichlorobenzene (250 mL) were stirred at 170 °C for 4 h. After cooling, the solvent was removed under vacuum. The residue was diluted with DCM, quenched with saturated aqueous NaHCO₃ and extracted with DCM. The combined organic phases were dried over MgSO₄, filtered, and concentrated. The residual solid was triturated with petroleum ether and dried under vacuum at 40 °C to afford **37** or **38**.

5.1.38. 4-bromo-7-methoxy-3-(4-methoxyphenyl)-2H-chromen-2-one (**37**)

Gray solid, yield 78.6%, MS (ESI) *m/z*: 360.1[M+H]⁺.

5.1.39. 4-bromo-7-methoxy-3-(4-fluorinephenyl)-2H-chromen-2-one (**38**)

Gray solid, yield 81.2%, ¹H (300 MHz, CDCl₃) δ (ppm): 7.88 (d, *J* = 8.9 Hz, 1H), 7.47 - 7.37 (m, 2H), 7.20 (t, *J* = 8.6 Hz, 2H), 6.98 (d, *J* = 8.8 Hz, 1H), 6.90 (s, 1H), 3.96 (s, 3H). MS (ESI) *m/z*: 370.1[M+Na]⁺.

5.1.40. General procedure for compounds **39a-d** and **40a-d**

Various basic side chains **35a-d** (1.0 mmol) was added to **37** (359 mg, 1.0 mmol) or **38** (347 mg, 1 mmol) in MeCN (10 mL). Cs₂CO₃ (636 mg, 2.0 mmol) was added, and the solution was stirred at 70 °C for 2-3 h. The mixture was allowed to cool, poured into water, and extracted with EtOAc twice. The combined extracts were dried over NaSO₄, filtered, and evaporated. The residue was purified by flash silica chromatography to give desired compounds **39a-d** and **40a-d** respectively.

5.1.41. 4-(4-(2-(dimethylamino)ethoxy)phenoxy)-7-methoxy-3-(4-methoxyphenyl)-2H-chromen-2-one (**39a**)

Light gray solid, yield 79.7%, mp 89-91°C; ¹H (300 MHz, CDCl₃) δ (ppm): 7.49 (d, *J* = 8.9 Hz, 1H), 7.33 - 7.26 (m, 2H), 6.86 (d, *J* = 2.4 Hz, 1H), 6.81 - 6.73 (m, 3H), 6.70 (s, 4H), 3.94 (t, *J* = 5.7 Hz, 2H), 3.85 (s, 3H), 3.74 (s, 3H), 2.67 (t, *J* = 5.7 Hz, 2H), 2.30 (s, 6H). ¹³C NMR (75 MHz, CDCl₃) δ: 162.7, 162.4, 158.8, 158.5, 154.2, 153.9, 150.2, 131.0, 124.9, 122.5, 116.6, 114.9, 114.2, 112.9, 111.9,

109.9, 100.1, 65.9, 57.7, 55.3, 54.7, 45.3. MS (ESI) m/z : 484.1 ($[M+Na]^+$). HRMS (ESI) for $C_{27}H_{27}NO_6+H$ calcd 462.1911, found 462.1915.

5.1.42. 4-(4-(2-(diethylamino)ethoxy)phenoxy)-7-methoxy-3-(4-methoxyphenyl)-2H-chromen-2-one (**39b**)

Light gray solid, yield 74.3%, mp 73-75°C; 1H (300 MHz, $CDCl_3$) δ (ppm): 7.50 (d, $J = 8.9$ Hz, 1H), 7.30 (d, $J = 8.8$ Hz, 2H), 6.87 (d, $J = 2.3$ Hz, 1H), 6.83 – 6.74 (m, 3H), 6.74 – 6.64 (m, 4H), 3.92 (t, $J = 6.2$ Hz, 2H), 3.86 (s, 3H), 3.75 (s, 3H), 2.80 (t, $J = 6.2$ Hz, 2H), 2.60 (q, $J = 7.1$ Hz, 4H), 1.04 (t, $J = 7.1$ Hz, 6H). ^{13}C NMR (75 MHz, $CDCl_3$) δ : 162.7, 162.4, 158.8, 158.5, 154.2, 154.1, 150.1, 131.0, 124.9, 122.5, 116.56, 114.9, 114.2, 112.9, 111.96, 109.9, 100.1, 66.5, 55.3, 54.7, 51.2, 47.3, 11.3. MS (ESI) m/z : 512.1 ($[M+Na]^+$). HRMS (ESI) for $C_{29}H_{31}NO_6+H$ calcd 490.2224, found 490.2225.

5.1.43. 7-methoxy-3-(4-methoxyphenyl)-4-(4-(2-(pyrrolidin-1-yl)ethoxy)phenoxy)-2H-chromen-2-one (**39c**)

Light yellow solid, yield 77.4%, mp 81-83°C; 1H (300 MHz, $CDCl_3$) δ (ppm): 7.49 (d, $J = 8.9$ Hz, 1H), 7.30 (d, $J = 8.9$ Hz, 2H), 6.87 (d, $J = 2.3$ Hz, 1H), 6.82 – 6.73 (m, 3H), 6.70 (s, 4H), 3.98 (t, $J = 5.9$ Hz, 2H), 3.85 (s, 3H), 3.74 (s, 3H), 2.83 (t, $J = 5.9$ Hz, 2H), 2.59 (s, 4H), 1.78 (dt, $J = 6.5, 3.2$ Hz, 4H). ^{13}C NMR (75 MHz, $CDCl_3$) δ : 162.7, 162.41, 158.8, 158.5, 154.2, 154.0, 150.2, 131.0, 124.9, 122.5, 116.6, 114.9, 114.2, 112.9, 111.9, 109.9, 100.1, 67.0, 55.29, 54.7, 54.5, 54.2, 22.9. MS (ESI) m/z : 510.1 ($[M+Na]^+$). HRMS (ESI) for $C_{29}H_{29}NO_6+H$ calcd 488.2088, found 488.2074.

5.1.44. 7-methoxy-3-(4-methoxyphenyl)-4-(4-(2-(piperidin-1-yl)ethoxy)phenoxy)-2H-chromen-2-one (**39d**)

Light brown solid, yield 85.9%, mp 95-97°C; 1H (300 MHz, $CDCl_3$) δ (ppm): 7.49 (d, $J = 8.9$ Hz, 1H), 7.34 – 7.27 (m, 2H), 6.87 (d, $J = 2.4$ Hz, 1H), 6.82 – 6.74 (m, 3H), 6.71 (dd, $J = 8.7, 2.7$ Hz, 4H), 3.98 (t, $J = 6.0$ Hz, 2H), 3.86 (s, 3H), 3.75 (s, 3H), 2.69 (t, $J = 6.0$ Hz, 2H), 2.52 – 2.41 (m, 4H), 1.59 (dt, $J = 10.9, 5.6$ Hz, 4H), 1.48 – 1.37 (m, 2H). ^{13}C NMR (75 MHz, $CDCl_3$) δ : 162.7, 162.4, 158.8, 158.5, 154.2, 154.0, 150.2, 131.0, 124.9, 122.5, 116.6, 115.0, 114.2, 112.9, 111.9, 109.9, 100.1, 65.9, 57.4, 55.3, 54.7, 54.6, 25.4, 23.7. MS (ESI) m/z : 524.1 ($[M+Na]^+$). HRMS (ESI) for $C_{30}H_{31}NO_6+H$ calcd 502.2224, found 502.2233.

5.1.45. 4-(4-(2-(dimethylamino)ethoxy)phenoxy)-3-(4-fluorophenyl)-7-methoxy-2H-chromen-2-one (**40a**)

Light brown solid, yield 81.3%, mp 73-76°C; 1H (300 MHz, $CDCl_3$) δ (ppm): 7.54 (d, $J = 8.9$ Hz, 1H), 7.35 – 7.26 (m, 2H), 6.96 – 6.85 (m, 3H), 6.79 (dd, $J = 8.9, 2.4$ Hz, 1H), 6.68 (s, 4H), 3.93 (t, $J = 5.7$ Hz, 2H), 3.85 (s, 3H), 2.66 (t, $J = 5.7$ Hz, 2H), 2.30 (s, 6H). ^{13}C NMR (75 MHz, $CDCl_3$) δ : 163.4, 162.7, 162.4, 160.1, 159.4, 154.3, 154.2, 149.9, 131.8, 131.6, 126.32, 126.3, 125.0, 116.7, 114.9, 114.5, 114.3, 112.9, 112.1, 109.7, 100.1, 65.9, 57.7, 55.3, 45.3. MS (ESI) m/z : 472.1 ($[M+Na]^+$). HRMS (ESI)

for C₂₆H₂₄FNO₅+H calcd 450.1822, found 450.1807.

5.1.46. 4-(4-(2-(diethylamino)ethoxy)phenoxy)-3-(4-fluorophenyl)-7-methoxy-2H-chromen-2-one (**40b**)

Light brown solid, yield 76.7%, mp 70-72°C; ¹H (300 MHz, CDCl₃) δ (ppm): 7.55 (d, *J* = 8.9 Hz, 1H), 7.32 (dd, *J* = 8.8, 5.4 Hz, 2H), 6.99 – 6.87 (m, 3H), 6.80 (dd, *J* = 8.9, 2.4 Hz, 1H), 6.68 (s, 4H), 3.98 – 3.86 (m, 5H), 2.81 (t, *J* = 6.2 Hz, 2H), 2.61 (q, *J* = 7.1 Hz, 4H), 1.05 (t, *J* = 7.1 Hz, 6H). ¹³C NMR (75 MHz, CDCl₃) δ: 163.5, 162.8, 162.5, 160.2, 159.40, 154.4, 154.2, 149.9, 131.7, 131.6, 126.3, 126.2, 125.1, 116.7, 114.9, 114.6, 114.3, 112.2, 109.8, 100.2, 66.6, 55.3, 51.2, 47.3, 11.3. MS (ESI) *m/z*: 500.1 ([M+Na]⁺). HRMS (ESI) for C₂₈H₂₈FNO₅+H calcd 478.2024, found 478.2031.

5.1.47. 3-(4-fluorophenyl)-7-methoxy-4-(4-(2-(pyrrolidin-1-yl)ethoxy)phenoxy)-2H-chromen-2-one (**40c**)

Light yellow solid, yield 68.4%, mp 88-91°C; ¹H (300 MHz, CDCl₃) δ (ppm): 7.53 (d, *J* = 8.9 Hz, 1H), 7.31 (dd, *J* = 8.8, 5.4 Hz, 2H), 6.97 – 6.85 (m, 3H), 6.78 (dd, *J* = 8.9, 2.4 Hz, 1H), 6.68 (s, 4H), 3.97 (t, *J* = 5.9 Hz, 2H), 3.85 (s, 3H), 2.82 (t, *J* = 5.9 Hz, 2H), 2.61 – 2.53 (m, 4H), 1.78 (dt, *J* = 6.6, 3.1 Hz, 4H). ¹³C NMR (75 MHz, CDCl₃) δ: 163.9, 163.2, 160.6, 159.9, 154.8, 154.7, 150.4, 132.2, 132.1, 126.8, 126.8, 125.6, 117.3, 115.5, 115.1, 114.8, 113.5, 112.7, 110.2, 100.6, 67.6, 55.8, 55.0, 54.7, 23.5. MS (ESI) *m/z*: 498.1 ([M+Na]⁺). HRMS (ESI) for C₂₈H₂₆FNO₅+H calcd 476.1868, found 476.1872.

5.1.48. 3-(4-fluorophenyl)-7-methoxy-4-(4-(2-(piperidin-1-yl)ethoxy)phenoxy)-2H-chromen-2-one (**40d**)

Brown solid, yield 84.8%, mp 109-111°C; ¹H (300 MHz, CDCl₃) δ (ppm): 7.54 (d, *J* = 8.9 Hz, 1H), 7.35 – 7.28 (m, 2H), 6.97 – 6.86 (m, 3H), 6.79 (dd, *J* = 8.9, 2.4 Hz, 1H), 6.68 (s, 4H), 3.97 (t, *J* = 6.0 Hz, 2H), 3.87 (s, 3H), 2.69 (t, *J* = 6.0 Hz, 2H), 2.51 – 2.41 (m, 4H), 1.58 (dt, *J* = 10.9, 5.6 Hz, 4H), 1.43 (dd, *J* = 11.1, 5.8 Hz, 2H). ¹³C NMR (75 MHz, CDCl₃) δ: 163.4, 162.7, 162.5, 160.2, 159.4, 154.4, 154.2, 149.9, 131.7, 131.6, 126.3, 126.3, 125.1, 116.7, 115.0, 114.6, 114.3, 113.1, 112.1, 109.7, 100.1, 66.0, 57.4, 55.3, 54.6, 25.4, 23.7. MS (ESI) *m/z*: 512.1 ([M+Na]⁺). HRMS (ESI) for C₂₉H₂₈FNO₅+H calcd 490.2024, found 490.2027.

5.1.49. General synthesis of final compounds **41a-d** and **42a-d**

Final compounds **41a-d** and **42a-d** were prepared according to General method III: demethylation.

5.1.50. 4-(4-(2-(dimethylamino)ethoxy)phenoxy)-7-hydroxy-3-(4-hydroxyphenyl)-2H-chromen-2-one (**41a**)

Yellow solid, yield 42.3%, mp 142-146°C; ¹H (300 MHz, DMSO) δ (ppm): 7.31 (d, *J* = 8.7 Hz, 1H), 7.18 (d, *J* = 8.6 Hz, 2H), 6.88 (d, *J* = 9.1 Hz, 2H), 6.77 (ddd, *J* = 11.0, 8.2, 2.2 Hz, 4H), 6.68 (d, *J* = 8.6 Hz, 2H), 3.95 (t, *J* = 5.7 Hz, 2H), 2.60 (t, *J* = 5.7 Hz, 2H), 2.22 (s, 6H). ¹³C NMR (75 MHz, DMSO) δ: 162.7, 161.9, 158.3, 157.4, 154.8, 154.3, 150.9, 131.8, 125.8, 121.8, 117.1, 115.8, 114.9,

113.7, 108.8, 102.7, 66.4, 58.0, 45.9. MS (ESI) m/z : 456.1 ($[M+Na]^+$). HRMS (ESI) for $C_{25}H_{23}NO_6+H$ calcd 434.1598, found 434.1604.

5.1.51. 4-(4-(2-(diethylamino)ethoxy)phenoxy)-7-hydroxy-3-(4-hydroxyphenyl)-2H-chromen-2-one (**41b**)

Yellow solid, yield 46.5%, mp 128-131°C; 1H (300 MHz, DMSO) δ (ppm): 7.28 (d, $J = 8.7$ Hz, 1H), 7.15 (d, $J = 8.6$ Hz, 2H), 6.82 (dd, $J = 13.5, 5.6$ Hz, 3H), 6.79 – 6.68 (m, 3H), 6.65 (d, $J = 8.6$ Hz, 2H), 3.92 (t, $J = 5.9$ Hz, 2H), 2.79 (t, $J = 5.8$ Hz, 2H), 2.59 (q, $J = 7.1$ Hz, 4H), 0.96 (t, $J = 7.1$ Hz, 6H). ^{13}C NMR (75 MHz, DMSO) δ : 162.2, 161.4, 157.8, 156.9, 154.3, 153.8, 150.4, 131.3, 125.2, 121.3, 116.7, 115.4, 114.5, 114.5, 113.1, 108.3, 102.2, 66.1, 51.1, 46.9, 11.3. MS (ESI) m/z : 484.1 ($[M+Na]^+$). HRMS (ESI) for $C_{27}H_{27}NO_6+H$ calcd 462.1911, found 462.1916.

5.1.52. 7-hydroxy-3-(4-hydroxyphenyl)-4-(4-(2-(pyrrolidin-1-yl)ethoxy)phenoxy)-2H-chromen-2-one (**41c**)

Yellow solid, yield 42.1%, mp 144-147°C; 1H (300 MHz, DMSO) δ (ppm): 7.26 (d, $J = 8.8$ Hz, 1H), 7.13 (d, $J = 8.5$ Hz, 2H), 6.83 (d, $J = 9.1$ Hz, 2H), 6.76 (d, $J = 4.7$ Hz, 2H), 6.74 – 6.66 (m, 2H), 6.63 (d, $J = 8.5$ Hz, 2H), 3.92 (s, 2H), 2.72 (s, 2H), 2.48 (s, 4H), 1.64 (s, 4H). ^{13}C NMR (75 MHz, DMSO) δ : 162.7, 161.9, 158.3, 157.4, 154.8, 154.3, 150.9, 131.8, 125.8, 121.8, 117.1, 115.8, 114.9, 113.7, 108.8, 102.7, 67.3, 54.7, 54.4, 23.6. MS (ESI) m/z : 482.1 ($[M+Na]^+$). HRMS (ESI) for $C_{27}H_{25}NO_6+H$ calcd 460.1755, found 460.1763.

5.1.53. 7-hydroxy-3-(4-hydroxyphenyl)-4-(4-(2-(piperidin-1-yl)ethoxy)phenoxy)-2H-chromen-2-one (**41d**)

Yellow solid, yield 48.3%, mp 155-158°C; 1H (300 MHz, DMSO) δ (ppm): 9.57 (s, 1H), 7.30 (d, $J = 8.7$ Hz, 1H), 7.18 (d, $J = 8.7$ Hz, 2H), 6.88 (d, $J = 9.2$ Hz, 2H), 6.85 – 6.80 (m, 2H), 6.79 – 6.72 (m, 2H), 6.68 (d, $J = 8.7$ Hz, 2H), 4.01 (t, $J = 5.6$ Hz, 3H), 2.73 (s, 2H), 2.53 (s, 2H), 1.52 (d, $J = 4.9$ Hz, 4H), 1.40 (d, $J = 4.7$ Hz, 2H). ^{13}C NMR (75 MHz, DMSO) δ : 162.7, 161.8, 158.2, 157.4, 154.8, 154.2, 150.9, 131.8, 125.8, 121.8, 117.1, 115.9, 115.1, 114.9, 113.6, 108.8, 102.7, 65.8, 57.4, 54.5, 25.5, 23.9. MS (ESI) m/z : 496.1 ($[M+Na]^+$). HRMS (ESI) for $C_{28}H_{27}NO_6+H$ calcd 474.1911, found 474.1914.

5.1.54. 4-(4-(2-(dimethylamino)ethoxy)phenoxy)-3-(4-fluorophenyl)-7-hydroxy-2H-chromen-2-one (**42a**)

White solid, yield 41.2%, mp 189-191°C; 1H (300 MHz, DMSO) δ (ppm): 7.37 (dd, $J = 13.3, 5.2$ Hz, 3H), 7.12 (td, $J = 8.9, 2.5$ Hz, 2H), 6.90 (dd, $J = 9.1, 2.5$ Hz, 2H), 6.83 (d, $J = 2.3$ Hz, 1H), 6.82 – 6.72 (m, 3H), 3.99 – 3.91 (m, 2H), 2.62 – 2.55 (m, 2H), 2.25 – 2.17 (m, 6H). ^{13}C NMR (75 MHz, DMSO) δ : 163.6, 162.5, 162.4, 160.3, 159.3, 155.1, 154.5, 150.7, 132.9, 132.8, 128.0, 125.9, 117.5, 115.9, 115.17, 114.88, 113.8, 113.5, 108.5, 102.8, 66.5, 58.0, 45.9. MS (ESI) m/z : 458.1 ($[M+Na]^+$). HRMS (ESI) for $C_{25}H_{22}FNO_5+H$ calcd 436.1555, found 436.1559.

5.1.55. 4-(4-(2-(diethylamino)ethoxy)phenoxy)-3-(4-fluorophenyl)-7-hydroxy-2H-chromen-2-one (42b)

Yellow solid, yield 38.6%, mp 121-125°C; ¹H (300 MHz, DMSO) δ (ppm): 7.42 – 7.34 (m, 3H), 7.11 (t, *J* = 8.9 Hz, 2H), 6.93 – 6.86 (m, 2H), 6.84 (d, *J* = 2.2 Hz, 1H), 6.80 – 6.73 (m, 3H), 3.92 (t, *J* = 6.1 Hz, 2H), 2.74 (t, *J* = 6.0 Hz, 2H), 2.59 – 2.53 (m, 4H), 0.97 (t, *J* = 7.1 Hz, 6H). ¹³C NMR (75 MHz, DMSO) δ: 163.6, 162.5, 162.4, 160.3, 159.3, 155.1, 154.5, 150.7, 132.9, 132.8, 128.0, 125.9, 117.5, 115.9, 115.17, 114.88, 113.8, 113.5, 108.5, 102.8, 66.5, 58.0, 45.9. MS (ESI) *m/z*: 486.1 ([M+Na]⁺). HRMS (ESI) for C₂₇H₂₆FNO₅+H calcd 464.1868, found 464.1873.

5.1.56. 3-(4-fluorophenyl)-7-hydroxy-4-(4-(2-(pyrrolidin-1-yl)ethoxy)phenoxy)-2H-chromen-2-one (42c)

Yellow solid, yield 44.5%, mp 109-111°C; ¹H (300 MHz, DMSO) δ (ppm): 7.45 – 7.33 (m, 3H), 7.12 (t, *J* = 8.9 Hz, 2H), 6.91 (d, *J* = 9.1 Hz, 2H), 6.85 (d, *J* = 2.1 Hz, 1H), 6.83 – 6.74 (m, 3H), 3.98 (t, *J* = 5.7 Hz, 2H), 2.79 (t, *J* = 5.7 Hz, 2H), 2.53 (dd, *J* = 5.8, 4.2 Hz, 4H), 1.69 (s, 4H). ¹³C NMR (75 MHz, DMSO) δ: 163.1, 161.9, 159.8, 158.8, 154.6, 153.9, 150.2, 132.4, 132.2, 127.5, 125.5, 117.0, 115.4, 114.7, 114.4, 113.3, 113.1, 108.1, 102.3, 66.8, 54.1, 53.9, 23.0. MS (ESI) *m/z*: 482.1 ([M+Na]⁺). HRMS (ESI) for C₂₇H₂₄FNO₅+H calcd 462.1711, found 462.1715.

5.1.57. 3-(4-fluorophenyl)-7-hydroxy-4-(4-(2-(piperidin-1-yl)ethoxy)phenoxy)-2H-chromen-2-one (42d)

Yellow solid, yield 48.4%, mp 116-118°C; ¹H (300 MHz, DMSO) δ (ppm): 7.43 – 7.33 (m, 3H), 7.11 (dd, *J* = 12.4, 5.5 Hz, 2H), 6.93 – 6.86 (m, 2H), 6.84 (d, *J* = 2.2 Hz, 1H), 6.82 – 6.73 (m, 3H), 3.96 (t, *J* = 5.8 Hz, 2H), 2.61 (t, *J* = 5.8 Hz, 2H), 2.41 (d, *J* = 4.9 Hz, 4H), 1.48 (dd, *J* = 10.2, 5.1 Hz, 4H), 1.38 (d, *J* = 4.7 Hz, 2H). ¹³C NMR (75 MHz, DMSO) δ: 163.6, 162.5, 162.4, 160.3, 159.3, 155.1, 154.5, 150.7, 132.8, 132.7, 127.9, 127.9, 125.9, 117.5, 115.9, 115.2, 114.9, 113.8, 113.6, 108.6, 102.8, 66.3, 57.7, 54.8, 25.9, 24.3. MS (ESI) *m/z*: 498.1 ([M+Na]⁺). HRMS (ESI) for C₂₈H₂₆FNO₅+H calcd 476.1868, found 476.1876.

5.2 Biological evaluation

5.2.1. ERα Binding Affinity Assay.

The recombinant ERα (Thermo Fisher Scientific Inc., Invitrogen, USA) and the fluorescent estrogen ligands (self-made) were removed from the -80°C freezer and thawed on ice for 1h prior to use. The fluorescent estrogen ligand was added to the ERα and screening buffer (ES2 Screening Buffer, Invitrogen, USA) was added to make the final concentration 9 nM for fluorescent estrogen and 30 nM for ERα. Test compounds were accurately weighed and dissolved in DMSO, screening buffer was added to dilute to required concentration. Test compound (1 μL) was added to 49 μL screening buffer in each well (384-well microplate, Corning, USA). To this 50 μL of the fluorescent estrogen/ER complex

was added to make up a final volume of 100 μL . A positive control contained 50 μL estradiol buffer (1nM) and 50 μL fluorescent estrogen/ER complex. A negative control contained 50 μL screening buffer and 50 μL fluorescent estrogen/ER complex. The negative control was used to determine the polarization value when no competitor was present (theoretical maximum polarization). The microplate was incubated in the dark at room temperature for 2 h and shaken on a plate shaker. The polarization values were read on a Safire microplate reader and used to calculate the IC_{50} values.

5.2.2. MTT assay for anti-proliferative activities

Cells were cultured in RPMI1640 medium (containing 10% (v/v) FBS, 100 U/mL Penicillin and 100 mg/mL Streptomycin) in a 5% CO_2 -humidified atmosphere at 37°C. Cells were trypsinized and seeded at a density of $1 \times 10^5/\text{mL}$ into a 96-well plate (100 $\mu\text{L}/\text{well}$) and incubated at 37°C, 5% CO_2 atmosphere for 24 h. After this time they were treated with 100 $\mu\text{L}/\text{well}$ medium containing test compounds which had been pre-prepared to provide the concentration range of 8×10^{-5} mol/L, 4×10^{-5} mol/L, 2×10^{-5} mol/L, 1×10^{-5} mol/L, 4×10^{-6} mol/L, 1×10^{-6} mol/L and 1×10^{-7} mol/L, and re-incubated for a further 48 h. Control wells were added the equivalent volume of medium containing 1% (v/v) DMSO. 20 μL MTT (5 mg/mL) was added and cells continued to incubate in darkness at 37°C for 4 h. The culture medium was then removed carefully and 150 μL DMSO was added. The cells were maintained at room temperature in darkness for 20 min to ensure thorough color diffusion before reading the absorbance. The absorbance values were read at 490 nm for determination of IC_{50} values.

5.2.3. VEGFR-2 Kinase Inhibitory Assay

VEGFR-2 kinase assay was conducted using homogeneous time resolved fluorescence (HTRF) assay. The general procedures were as following: VEGFR-2 kinase (Invitrogen, USA), substrates, ATP and test compounds were mixed and incubated in a final buffer with the total volume of 10 μL in 384-well microplate. Wells containing the substrate and the kinase without compound were used as total reaction control. The assay plate was incubated at 30°C in the dark for 1 h. Detection was performed with HTRF module of Beckman Coulter detection platform to get the fluorescence values which were further used to calculate the percentage inhibition values.

5.2.4. Cell migration assay

Cell migration assay were carried out using 24-well plate and wound-healing method. Briefly, MCF-7 cells were seeded in a 24-well plate and were allowed to grow to 100% confluence. Cell culture were injured by a 10 mL tip, cells were washed twice with PBS, and then incubated with fresh medium with or without compound **42d** at different concentrations for 24 and 48 h. Cell migration to the damaged area was then visualized and photographed on a phase contrast microscope.

5.2.5. Cell cycle analysis

The MCF-7 cells were treated with 2 μ M, 4 μ M and 6 μ M of **42d** for 24 h. After treatment, the cells were washed twice with ice-cold PBS, collected by centrifugation, and fixed in ice-cold 70% (v/v) ethanol, washed with PBS, re-suspended with 0.1 mg/mL RNase, stained with 40 mg/mL PI, and analyzed by flow cytometry using FACScalibur (Becton Dickinson). The cell cycle distributions were calculated using Flowjo 7.6.1 software.

5.2.6. Real-Time Polymerase Chain Reaction (RT-PCR).

RNA samples were reverse transcribed to cDNA and the PCR reactions were performed using TaKaRa SYBR Green Master Mix (Code. no. 638320) carried out in StepOnePlus™ Real-Time PCR instrument (4376600, Life Technologies). The program for amplification was 1 cycle of 95°C for 2 min followed by 40 cycles of 95°C for 10 s, 60°C for 30 s, and 95°C for 10 s. The PCR results were normalized to GAPDH expression and were quantified by the $\Delta\Delta$ CT method.

5.2.7. Western Blots.

Cells with different treatments for 24h were washed twice with PBS, then collected and lysed in lysis buffer (100 mM of Tris-Cl, pH 6.8, 4% (m/v) SDS, 20% (v/v) glycerol, 200 mM of β -mercaptoethanol, 1mM of PMSF, 0.1 mM NaF and DTT) for 1 h on the ice. The lysates were then subjected to centrifugation (13,000 rpm) at 4 °C for 20 min. Protein concentration in the supernatants was detected by BCA protein assay (Thermo, Waltham, MA). Then equal amount of protein was separated with 12% SDS-PAGE and transferred to polyvinylidene difluoride (PVDF) membranes (Millipore, Bedford, MA) using a semi-dry transfer system (Bio-rad, Hercules, CA). Proteins were detected using specific antibodies overnight at 4 °C followed by HRP-conjugated secondary antibodies for 1 h at 37 °C. All of the antibodies were diluted in PBST containing 1% BSA. Enhanced chemiluminescent reagents (Beyotime, Jiangsu, China) were used to detect the HRP on the immunoblots, and the visualized bands were captured by film. The bands were quantified by Quantity One software (Vision 4.62, Bio-rad, Hercules, CA), and the relative protein level were normalized to β -actin.

5.2.8. Molecular modeling

The molecular modeling was performed with Discovery Studio.3.0/CDOCK protocol (*Accelrys Software Inc.*). The crystal structures of ER α complexed with 4-hydroxytamoxifen (PDB code: 3ERT) and VEGFR-2 (PDB ID code: 1YWN) were downloaded from Protein Data Bank. Compounds **17d**, **23d**, **29d**, **30d**, **39d**, **40d**, **41d** and **42d** were drawn and optimized. The protein and ligand were optimized and charged to perform docking. Up to 10 conformations were retained, and binding modes presented graphically are representative of the highest-scored conformations.

Supplementary data

Supplementary data (the ^1H NMR, ^{13}C NMR and HRMS spectra of target compounds associated with this article can be found, in the online version, at.

Acknowledgements

This work was supported by grants from the Natural Science Foundation of China (NSFC, 81373279) and the Twelfth Five-Year Plan Major Project of Candidate Drugs (Ministry of National Science and Technology, 2012ZX09103101048). The authors are grateful to *Nanjing Paopao Biotechnology Co., Ltd* for performing the Western Blot experiment.

Abbreviations

ER, estrogen receptor; SERMs, selective estrogen receptor modulators; V2-I, VEGFR-2 inhibitor; HDAC, histone deacetylases; VEGF, Vascular endothelial growth factor; VEGFR-2, Vascular endothelial growth factor receptor-2; RTK, receptor tyrosine kinase; MAPK, mitogen-activated protein kinase; ERK, extracellular regulated kinases; HUVEC, human umbilical vein endothelial cell; RT-PCR, real-time polymerase chain reaction; PgR, progesterone receptor; E2, estradiol; SAR, structure-activity relationship; MTT, 3-(4,5-dimethylthiazol-2-yl)-2,5-diphenyltetrazolium bromide.

References and notes

- [1] M.H. Forouzanfar, K.J. Foreman, A.M. Delossantos, R. Lozano, A.D. Lopez, C.J.L. Murray, M. Naghavi, Breast and cervical cancer in 187 countries between 1980 and 2010: a systematic analysis, *Lancet* 378 (2011) 1461-1484.
- [2] I.A. Mohd, K.H. Mohd, A. Ashutosh, C. Bandana, K. Rituraj, K. Hajela, Synthesis of targeted dibenzo[b,f]thiepinines and dibenzo[b,f]oxepines as potential lead molecules with promising anti-breast cancer activity, *Eur. J. Med. Chem.* 99 (2015) 113-124.
- [3] T. Traboulsi, M.E. Ezzy, J.L. Gleason, S. Mader, Antiestrogens: structure-activity relationships and use in breast cancer treatment, *J. Mol. Endocrinol* 58 (2017) 15-31.
- [4] M.A. Feitelson, A. Arzumanyan, R.J. Kulathinal, S.W. Blain, R.F. Holcombe, J. Mahajna, M. Marino, M.L. Martinez-Chantar, R. Nawroth, I. Sanchez-Garcia, et al, Sustained proliferation in cancer: Mechanisms and novel therapeutic targets, *Seminars in Cancer Biology* 35 (2015) 25-54.
- [5] S. E. Amir, O.C. Freedman, B. Seruga, D.G. Evans, Assessing Women at High Risk of Breast Cancer: A Review of Risk Assessment Models, *J. Natl. Cancer Inst.* 102 (2010), 680-691.
- [6] C. Maurer, S. Martel, D. Zardavas, M. Ignatiadis, New agents for endocrine resistance in breast cancer, *The Breast* 34 (2017) 1-11.
- [7] T. Traboulsi, M.E. Ezzy1, J.L. Gleason, S. Mader, Antiestrogens: structure-activity relationships and use in breast cancer treatment, *Curr. Top. Med. Chem.* 58 (2017) 15-31.
- [8] K. Maruyama, M. Nakamura, S. Tomoshige, K. Sugita, M. Makishima, Y. Hashimoto, M. Ishikawa Structure-activity relationships of bisphenol A analogs at estrogen receptors (ERs): discovery of an ER α -selective antagonist, *Bioorg. Med. Chem. Lett.*, 23 (2013) 4031- 4036.
- [9] Z. Bai, R. Gust, Breast cancer, estrogen receptor and ligands, *Arch. Pharm.*, 342 (2009) 133-149.
- [10] G. Kaur, M.P. Mahajan, M.K. Pandey, P. Singh, S.R. Ramiseti, A.K. Sharma, Design, synthesis and evaluation of Ospemifene analogs as anti-breast cancer agents, *Eur. J. Med. Chem.* 86 (2014) 211-218.
- [11] V.C. Jordan, Chemoprevention of breast cancer with selective oestrogen-receptor modulators, *Nat. Rev. Cancer* 7 (2007) 46-53.
- [12] V.C. Jordan, R. McDaniel, F. Agboke, P.Y. Maximov, The evolution of nonsteroidal antiestrogens

- to become selective estrogen receptor modulators, *Steroids* 90 (2014) 3-12.
- [13] J.S. Lewis-Wambi, H. Kim, R. Curpan, R. Grigg, M.A. Sarker, V.C. Jordan, The Selective Estrogen Receptor Modulator Bazedoxifene Inhibits Hormone-Independent Breast Cancer Cell Growth and Down-Regulates Estrogen Receptor α and Cyclin D1, *Mol. Pharmacol.* 80 (2011) 610-620.
- [14] S.J. Han, K. Begum, C.E. Foulds, R.A. Hamilton, S. Bailey, A. Malovannaya, D. Chan, J. Qin, B.W. O'Malley, The Dual Estrogen Receptor α Inhibitory Effects of the Tissue-Selective Estrogen Complex for Endometrial and Breast Safety, *Mol. Pharmacol.* 89 (2016) 14-26.
- [15] T.L. Wang, Q.D. You, F.S.G. Huang, H. Xiang, Recent Advances in Selective Estrogen Receptor Modulators for Breast Cancer, *Mini-Rev. Med. Chem.* 9 (2009) 1191-1201.
- [16] J.A. Katzenellenbogen, The 2010 Philip S. Portoghese Medicinal Chemistry Lectureship: addressing the "core issue" in the design of estrogen receptor ligands, *J. Med. Chem.* 54 (2011) 5271-5282.
- [17] T.I. Richardson, S.A. Frank, M. Wang, C.A. Clarke, S.A. Jones, B.P. Ying, D.T. Kohlman, O.B. Wallace, T.A. Shepherd, R.D. Dally, Structure-activity relationships of SERMs optimized for uterine antagonism and ovarian safety, *Bioorg. Med. Chem. Lett.* 17 (2007) 3544-3549.
- [18] R.K. Gara, V. Sundram, S.C. Chauhan, M. Jaggi, Anti-cancer potential of a novel SERM ormeloxifene, *Curr Med Chem.* 20 (2013) 4177-4184.
- [19] I. Barretta, M.J. Meegana, R.B. Hughesa, M. Carra, A.J.S. Knox, N. Artemenkob, G. Golfish, D.M. Zistererc, D.G. Lloydb, Synthesis, biological evaluation, structural-activity relationship, and docking study for a series of benzoxepin-derived estrogen receptor modulators, *Bioorg. Med. Chem.* 16 (2008) 9554-9573.
- [20] N. Suzuki, X.P. Liu, Y.R. Santosh Laxmi, K. Okamoto, H. Jeong Kim, G.X. Zhang, J.J. Chen, Y. Okamoto, S. Shibutani, Anti-breast cancer potential of SS5020, a novel benzopyran antiestrogen, *INT. J. Cancer* 128 (2011) 974-982.
- [21] G.S. Luo, M.Q. Chen, W.T. Lyu, R.H. Zhao, Q. Xu, Q.D. You, H. Xiang, Design, synthesis, biological evaluation and molecular docking studies of novel 3-aryl-4-anilino-2H-chromen-2-one derivatives targeting ER α as anti-breast cancer agents, *Bioorg. Med. Chem. Lett.* 27 (2017) 2668-2673.
- [22] J.Y. Chen, S.J. Kuo, Y.P. Liaw, I. Avital, A. Stojadinovic, Y.G. Man, C. Mannion, J.L. Wang, M.C. Chou, H.D. Tsai, Endometrial Cancer Incidence in Breast Cancer Patients Correlating with Age and Duration of Tamoxifen Use: a Population Based Study, *J Cancer* 5 (2014) 151-155.
- [23] J. Peng, S. Sengupta, V.C. Jordan, Potential of selective estrogen receptor modulators as treatments and preventives of breast cancer. *Anticancer Agents Med Chem.* 9 (2009) 481-499.
- [24] R. Garcia-Becerra, N. Santos, L. Diaz, J. Camacho, Mechanisms of Resistance to Endocrine Therapy in Breast Cancer: Focus on Signaling Pathways, miRNAs and Genetically Based Resistance. *International journal of molecular sciences* 14 (2012) 108-145.
- [25] M. Droog, K. Beelen, S. Linn, W. Zwart, Tamoxifen resistance: from bench to bedside. *Eur J Pharmacol* 717 (2013) 45-57.
- [26] K. Dao, R.N. Hanson, Targeting the Estrogen Receptor using Steroid-Therapeutic Drug Conjugates (Hybrids), *Bioconjugate Chem.* 23 (2012) 2139-2158.
- [27] A. Gupta, P. Saha, C. Descôteaux, V. Leblanc, E. Asselin, G. Bérubé, Design, synthesis and biological evaluation of estradiol-chlorambucil hybrids as anticancer agents, *Bioorg. Med. Chem. Lett.* 20 (2010) 1614-1618.
- [28] N.M. O'Boyle, J.K. Pollock, M. Carr, A.J. Knox, S.M. Nathwani, S. Wang, L. Caboni, D.M. Zisterer, M.J. Meegan, beta-Lactam estrogen receptor antagonists and a dual-targeting estrogen receptor/tubulin ligand, *J. Med. Chem.* 57 (2014) 9370-9382.
- [29] C.H. Li, C. Tang, Z.Y. Hu, C.X. Zhao, C.L. Li, S.L. Zhang, C.N. Dong, H.B. Zhou, J. Huang, Synthesis and structure-activity relationships of novel hybrid ferrocenyl compounds based on a bicyclic core skeleton for breast cancer therapy, *Bioorg. Med. Chem.* 24 (2016) 3062-3074.
- [30] W. Lv, J.Z. Liu, T.C. Skaar, E. O'Neill, G. Yu, D.A. Flockhart, M. Cushman, Synthesis of Triphenylethylene Bisphenols as Aromatase Inhibitors That Also Modulate Estrogen Receptors, *J. Med. Chem.* 59 (2016) 157-170.
- [31] R.R. Patel, S. Sengupta, H.R. Kim, A.J. Klein-Szanto, J.R. Pyle, F. Zhu, T.Y. Li, E.A. Ross, S. Oseni, J. Fagnoli, V.C. Jordan, Experimental treatment of oestrogen receptor (ER) positive breast cancer with tamoxifen and brivanib alaninate, a VEGFR-2/FGFR-1 kinase inhibitor: A potential clinical application of angiogenesis inhibitors, *Eur. J. Cancer.* 46 (2010) 1537-1553.
- [32] J.E. Huh, Y.H. Baek, M.H. Lee, D.Y. Choi, D.S. Park, J.D. Lee, Bee venom inhibits tumor angiogenesis and metastasis by inhibiting tyrosine phosphorylation of VEGFR-2 in LLC-tumor-bearing mice, *Cancer. Lett.* 292 (2010) 98-110.

- [33] J.D. Yan, Y.R. Liu, Z.Y. Zhang, G.Y. Liu, J.H. Xu, L.Y. Liu, Y.M. Hu, Expression and prognostic significance of VEGFR-2 in breast cancer in tumor growth and angiogenesis, *Pathol. Res. Pract.* 211 (2015) 539-543.
- [34] D. Huang, Y. Ding, W.M. Luo, S. Bender, C.N. Qian, E. Kort, Z.F. Zhang, K. VandenBeldt, N.S. Duesbery, J.H. Resau, B.T. Teh, Inhibition of MAPK kinase signaling pathways suppressed renal cell carcinoma growth and angiogenesis in vivo, *Cancer Res.* 68 (2008) 81-88.
- [35] M.E. Fratto, M. Imperatori, B. Vincenzi, F. Tomao, D. Santini, G. Tonini, New perspectives: role of Sunitinib in Breast Cancer, *Clin. Ter.* 161 (2010) 475-482.
- [36] Z. Madak-Erdogan, M. Lupien, F. Stossi, M. Brown, B.S. Katzenellenbogen, Genomic collaboration of estrogen receptor alpha and extracellular signal-regulated kinase 2 in regulating gene and proliferation programs, *Mol. Cell. Biol.* 31 (2011) 226-236.
- [37] L.M. McGlynn, T. Kirkegaard, J. Edwards, S. Tovey, D. Cameron, C. Twelves, J.M. Bartlett, T.G. Cooke, Ras/Raf-1/MAPK pathway mediates response to tamoxifen but not chemotherapy in breast cancer patients, *Clin. Cancer Res.* 15 (2009) 1487-1495.
- [38] Z.C. Tang, S.X. Niu, F. Liu, K.J. Lao, J.S. Miao, J.Z. Ji, X. Wang, M. Yan, L.Y. Zhang, Q.D. You, H. Xiao, H. Xiang, Synthesis and biological evaluation of 2,3-diaryl isoquinolinone derivatives as anti-breast cancer agents targeting ER alpha and VEGFR-2, *Bioorg. Med. Chem. Lett.* 24 (2014) 2129-2133.
- [39] Z.C. Tang, C.Z. Wu, T.L. Wang, K.J. Lao, Y.J. Wang, L.Y. Liu, M. Muyaba, P. Xu, C.H. He, G.S. Luo, Z.Y. Qian, S.X. Niu, L.J. Wang, Y. Wang, H. Xiao, Q.D. You, H. Xiang, Design, synthesis and evaluation of 6-aryl-indenoisoquinolone derivatives dual targeting ER α and VEGFR-2 as anti-breast cancer agents, *Eur. J. Med. Chem.* 118 (2016) 328-339.
- [40] H. Chen, S. Li, Y.C. Yao, L.K. Zhou, J.P. Zhao, Y.J. Gu, K.R. Wang, X.L. Li, Design, synthesis, and anti-tumor activities of novel triphenylethylene-coumarin hybrids, and their interactions with Ct-DNA, *Bioorg. Med. Chem. Lett.* 23 (2013) 4785-4789.
- [41] W.J. Zhang, Z. Li, M. Zhou, F. Wu, X.Y. Hou, H. Luo, H. Liu, X. Han, G.Y. Yan, Z.Y. Ding, R. Li, Synthesis and biological evaluation of 4-(1,2,3-triazol-1-yl)coumarin derivatives as potential antitumor agents, *Bioorg. Med. Chem. Lett.* 24 (2014) 799-807.
- [42] X. Han, J. Luo, F. Wu, X.Y. Hou, G.Y. Yan, M. Zhou, M.Q. Zhang, C.L. Pu, R. Li, Synthesis and biological evaluation of novel 2,3-dihydrochromeno[3,4-d]imidazol-4(1H)-one derivatives as potent anticancer cell proliferation and migration agents, *Eur. J. Med. Chem.* 114 (2016) 232-243.
- [43] G.S. Luo, M. Muyaba, W.T. Lyu, Z.C. Tang, R.H. Zhao, Q. Xu, Q.D. You, H. Xiang, Design, synthesis and biological evaluation of novel 3-substituted 4-anilino-coumarin derivatives as antitumor agents, *Bioorg. Med. Chem. Lett.* 27 (2017) 867-874.
- [44] T.O. Olomola, R. Klein, N. Mautsa, Y. Sayed, P.T. Kaye, Synthesis and evaluation of coumarin derivatives as potential dual-action HIV-1 protease and reverse transcriptase inhibitors, *Bioorg. Med. Chem.* 21 (2013) 1964-1971.
- [45] A. Arshad, H. Osman, M.C. Bagley, C.K. Lam, S. Mohamad, A.S. Zahariluddin, Synthesis and antimicrobial properties of some new thiazolyl coumarin derivatives, *Eur. J. Med. Chem.* 46 (2011) 3788-3794.
- [46] L.Z. Chen, W.W. Sun, L. Bo, J.Q. Wang, C. Xiu, W.J. Tang, J.B. Shi, H.P. Zhou, X.H. Liu, New arylpyrazoline-coumarins: Synthesis and anti-inflammatory activity, *Eur. J. Med. Chem.* 138 (2017) 170-181.
- [47] A. Bisi, C. Cappadone, A. Rampa, G. Farruggia, A. Sargenti, F. Belluti, R.M. Di Martino, E. Malucelli, A. Meluzzi, S. Iotti, S. Gobbi, Coumarin derivatives as potential antitumor agents: Growth inhibition, apoptosis induction and multidrug resistance reverting activity, *Eur. J. Med. Chem.* 127 (2017) 577-585.
- [48] S. Emami, S. Dadashpour, Current developments of coumarin-based anti-cancer agents in medicinal chemistry, *Eur. J. Med. Chem.* 102 (2015) 611-630.
- [49] A. Thakur, R. Singla, V. Jaitak, Coumarins as anticancer agents: a review on synthetic strategies, mechanism of action and SAR studies, *Eur. J. Med. Chem.* 101 (2015) 476-495.
- [50] S. Sinha, A.P. Kumaran, D. Mishra, P. Paira, Synthesis and cytotoxicity study of novel 3-(triazolyl)coumarins based fluorescent scaffolds, *Bioorg. Med. Chem. Lett.*, 26 (2016) 5557-5561.
- [51] D. Cao, Y.B. Liu, W. Yan, C.Y. Wang, P. Bai, T.J. Wang, M.H. Tang, X.Y. Wang, Z. Yang, B.Y. Ma, L. Ma, L. Lei, F. Wang, B.X. Xu, Y.Y. Zhou, T. Yang, L.J. Chen, Design, Synthesis, and Evaluation of in Vitro and in Vivo Anticancer Activity of 4-Substituted Coumarins: A Novel Class of Potent Tubulin Polymerization Inhibitors, *J. Med. Chem.* 59 (2016) 5721-5739.
- [52] S. Lee, K. Sivakumar, W.S. Shin, F. Xie, Q. Wang, Synthesis and anti-angiogenesis activity of coumarin derivatives, *Bioorg. Med. Chem. Lett.* 16 (2006) 4596-4599.

- [53] R. Pan, Y. Dai, X.H. Gao, D. Lu, Y.F. Xia, Inhibition of vascular endothelial growth factor-induced angiogenesis by scopoletin through interrupting the autophosphorylation of VEGF receptor 2 and its downstream signaling pathways, *Vasc. Pharmacol.* 54 (2011) 18-28.
- [54] B.R. Vijay Avin, P. Thirusangu, V. Lakshmi Ranganatha, A. Firdouse, B.T. Prabhakar, S.A. Khanum, Synthesis and tumor inhibitory activity of novel coumarin analogs targeting angiogenesis and apoptosis, *Eur. J. Med. Chem.* 75 (2014) 211-221.
- [55] T.I. Richardson, S.A. Frank, M. Wang, C.A. Clarke, S.A. Jones, B.P. Ying, D.T. Kohlman, O.B. Wallace, T.A. Shepherd, R.D. Dally, A.D. Palkowitz, A.G. Geiser, H.U. Bryant, J.W. Henck, I.R. Cohen, D.G. Rudmann, D.J. McCann, D.E. Coutant, S.W. Oldham, C.W. Hummel, K.C. Fong, R. Hinklin, G. Lewis, H. Tian, J.A. Dodge, Structure-activity relationships of SERMs optimized for uterine antagonism and ovarian safety, *Bioorg. Med. Chem. Lett.* 17 (2007) 3544-3549.
- [56] Q.A. Huchet, B. Kuhn, B. Wagner, N.A. Kratochwil, H. Fischer, M. Kansy, D. Zimmerli, E.M. Carreira K. Müller, Fluorination Patterning: A Study of Structural Motifs That Impact Physicochemical Properties of Relevance to Drug Discovery, *J. Med. Chem.*, 58 (2015) 9041-9060.
- [57] I. Ojima, Strategic incorporation of fluorine into taxoid anticancer agents for medicinal chemistry and chemical biology studies, *J. Fluorine Chem.* 198 (2017) 10-23.
- [58] W.M. Eldehn, S.M. Abou-Seri, A.M. El Kerdawy, R.R. Ayyad, A.M. Hamdy, H.A. Ghabbour, M.M. Ali, D.A. A. El Ella, Increasing the binding affinity of VEGFR-2 inhibitors by extending their hydrophobic interaction with the active site: Design, synthesis and biological evaluation of 1-substituted-4-(4-methoxybenzyl) phthalazine derivatives, *Eur. J. Med. Chem.* 113 (2016) 50-62.
- [59] F.M. Yakes, J. Chen, J. Tan, K. Yamaguchi, Y. Shi, P. Yu, F. Qian, F. Chu, F. Bentzien, B. Cancilla, Cabozantinib (XL184), a novel MET and VEGFR2 inhibitor, simultaneously suppresses metastasis, angiogenesis, and tumor growth, *Mol. Cancer Ther.* 10 (2011) 2298-2308.
- [60] S.L. Degorce, A. Bailey, R. Callis, C. De Savi, R. Ducray, G. Lamont, P. MacFaul, M. Maudet, S. Martin, R. Morgentin, R.A. Norman, A. Peru, J.H. Pink, P.A. Plé, B. Roberts, J.S. Scott, Investigation of (E)-3-[4-(2-Oxo-3-aryl-chromen-4-yl)oxyphenyl]acrylic Acids as Oral Selective Estrogen Receptor Down-Regulators, *J. Med. Chem.* 58 (2015) 3522-3533.
- [61] A. Maiti, K. Takabe, N.C. Hait, Metastatic triple-negative breast cancer is dependent on SphKs/S1P signaling for growth and survival, *Cell Signal.* 32 (2017) 85-92.
- [62] L.J. Wang, Y. Wang, H.Q. Du, Y. Jiang, Z.C. Tang, H.Y. Liu, H. Xiang, H. Xiao, Impact of ER520, a candidate of selective estrogen receptor modulators, on in vitro cell growth, migration, invasion, angiogenesis and in vivo tumor xenograft of human breast cancer cells, *Cancer Chemother Pharmacol.* 76 (2015) 1247-1257.
- [63] V.L. Heath, R. Bicknell, Anticancer strategies involving the vasculature, *Nat. Rev. Clin. Oncol.* 6 (2009) 395-404.
- [64] S.C. Guo, L.S. Colbert, M. Fuller, Y.Y. Zhang, R.R. Gonzalez-Perez, Vascular endothelial growth factor receptor-2 in breast cancer, *Biochimica et Biophysica Acta.* 1806 (2010) 108-121.
- [65] A. Nardone, C. De Angelis, M.V. Trivedi, C.K. Osborne, R. Schiff, The changing role of ER in endocrine resistance, *The Breast* 24 (2015) 60-66.
- [66] L. Santarpia, S.M. Lippman, A.K. El-Naggar, Targeting the MAPK-RAS-RAF signaling pathway in cancer therapy, *Expert Opin. Ther. Tar.* 16 (2012) 103-119.
- [67] L.M. McGlynn, T. Kirkegaard, J. Edwards, S. Tovey, D. Cameron, C. Twelves, J.M. Bartlett, T.G. Cooke, Ras/Raf-1/MAPK pathway mediates response to tamoxifen but not chemotherapy in breast cancer patients, *Clin. Cancer Res.* 15 (2009) 1487-1495.
- [68] A. Arcaro, A.S. Guerreiro, The phosphoinositide 3-kinase pathway in human cancer: genetic alterations and therapeutic implications, *Curr. Genomics* 8 (2007) 271-306.
- [69] V.A. Machado, D. Peixoto, R. Costa, H.J.C. Froufe, R.C. Calhelha, R.M.V. Abreu, I.C.F.R. Ferreira, R. Soares, M.R.P. Queiroz, Synthesis, antiangiogenesis evaluation and molecular docking studies of 1-aryl-3-[(thieno[3,2-b]pyridin-7-ylthio)phenyl]ureas: Discovery of a new substitution pattern for type II VEGFR-2 Tyr kinase inhibitors, *Bioorg. Med. Chem.* 23 (2015) 6497-6509

Captions for figures, schemes and tables:

Captions for figures:

Figure 1. Previously reported selective estrogen receptor modulators (SERMs)

Figure 2. (A) Previously referenced dual-acting ER ligand conjugates (B) multiple ligands of ER α and VEGFR-2 together with outstanding biological results reported by our group previously

Figure 3. The rationally design of targeted compounds based on 3-aryl-4-anilino/aryloxy-2H-chromen-2-one scaffold. (A) Schematic representation of the catalytic pocket of ER α and the chemical modulation strategy. (B) Previously reported VEGFR-2 inhibitor and the design of novel inhibitor for VEGFR-2 kinase (C) Docking analysis of a putative compound **17d** within active site of VEGFR-2 (for clarity, only interacting residues are labeled. Hydrogen-bonding and hydrophobic interactions are shown by red dashes). (D) Schematic representation showing the overall designing strategy of dual ER α and VEGFR-2 ligands.

Figure 4. *In vitro* anti-proliferative properties of selected compounds against MCF-7 and Ishikawa cell lines. (A) Growth inhibition assay performed on MCF-7 and Ishikawa cell cells using MTT after 48 h incubation with a range of drug concentrations. Points: % of cell proliferation as compared to untreated control cells, means of at least three individual experiments. (B) Histogram representation of the micromolar concentration of the compounds required to inhibit 50% of MCF-7 and Ishikawa cell proliferation after 48 h drug incubation (IC₅₀). Columns: means of at least three individual experiments; bars: SD.

Figure 5. Effects on the migration of MCF-7. Representative images of MCF-7 cells treated with serum-free 1640 medium containing **42d** (2 and 4 μ M) for 24 and 48 h were photographed under phase contrast microscopy (magnification, 100 \times). Control was treated with serum-free 1640 medium.

Figure 6. (A) Cell cycle analysis of MCF-7 cells treatment of compound **42d** (2, 4 and 6 μ M) and Tamoxifen (2 μ M) as positive control for 24 h.

Figure 7. The increased mRNA expression of PR induced by E2 was reversed by **42d** in MCF-7 cells. The mRNA expression of PR was examined by Real-time PCR. Values are mean \pm SD (n=3). * P < 0.05, ** P < 0.01, *** P < 0.001 vs. E2 group. # P < 0.05, ## P < 0.01, ### P < 0.001.

Figure 8. **42d** inhibits the phosphorylation of VEGFR-2 in MCF-7 cells. (A) Expression of p-VEGFR-2 and VEGFR-2 in MCF-7 cells were examined by western blots. (B) Densitometric analysis was performed to determine the phosphorylation rate of VEGFR-2. Values are mean \pm SD (n = 3). *P < 0.05, **P < 0.01, ***P < 0.001 vs. Control group.

Figure 9. **42d** inhibits the activity of the Raf-1/ERK pathway in MCF-7 cells. (A) Expression of p-Raf-1, Raf-1, p-ERK1/2, and ERK1/2 were examined by western blots in MCF-7 cells. (B) Densitometric analysis was performed to determine the phosphorylation rate of Raf-1 and ERK1/2. Values are mean \pm SD (n = 3). *P < 0.05, **P < 0.01, ***P < 0.001 vs. Control group; #P < 0.05, ##P < 0.01, ###P < 0.001 vs. Control group.

Figure 10. Schematic representation elucidating the role of **42d** in interfering with signaling pathways initiated by ER α and VEGFR-2

Figure 11. (A) Superimposed poses of OHT (blue) with representative derivatives **42d** (yellow), binding to ER α , the protein was shown in surface. (B) Docking interactions of **42d** within ER α active site (surrounding residues shown as green sticks). Dotted lines (red) represent the hydrogen bonding interaction.

Figure 12. The binding mode of compound **42d** (ball and stick in yellow) docked into the

VEGFR-2 binding site (surrounding residues shown as gray sticks). Hydrogen bonding and hydrophobic interactions are shown as red dotted lines with distances in angstrom.

Captions for schemes:

Scheme 1. Synthetic routes of **17a-d**. Reagents and conditions: (a) K_2CO_3 , EtOH, 75 °C, 3 h; (b) BBr_3 , CH_2Cl_2 , rt, 12 h.

Scheme 2. Synthetic routes of **23a-d**. Reagents and conditions: (a) $POCl_3$, pyridine, 0-10 °C, 2 h; (b) KOH, pyridine, rt, 4 h; (c) TsCl, Et_3N , dry DCM, rt, 0.5 h; (d) arylamines, K_2CO_3 , EtOH, 75 °C, 2-3 h.

Scheme 3. Synthetic routes of **29a-d** and **30a-d**. Reagents and conditions: (a) $BF_3 \cdot OEt_2$, 85 °C, 2.5 h; (b) MeOH, PPh_3 , DIAD, THF, 0 °C-rt, 0.5 h; (c) NaH, DEC, 120 °C, 2 h; (d) TsCl, Et_3N , dry DCM, 0.5 h; (e) arylamines, K_2CO_3 , EtOH, 75 °C, 2-3 h; (f) BBr_3 , CH_2Cl_2 , rt, 12 h.

Scheme 4. Synthetic routes of **39a-d**, **40a-d**, **41a-d** and **42a-d**. Reagents and conditions: (a) K_2CO_3 , dry acetone, MOMCl, rt, 2 h; (b) 5N NaOH solution, $ClCH_2CH_2Cl$, TBAB, 75 °C, 4 h; (c) RCl or RCl·HCl, K_2CO_3 , KI, DMF, 100 °C, 4 h; (d) concentrated HCl, MeOH, rt, 4 h; (e) $POBr_3$ (1.1 equiv), 1,2-dichlorobenzene, 170 °C, 4 h; (f) arylamines, Cs_2CO_3 (2 equiv), MeCN, 75 °C, 2-3 h; (g) BBr_3 , CH_2Cl_2 , rt, 12 h.

Captions for tables:

Table 1 SAR of C-4 substituted N-aryl analogs **17a-d**, **23a-d**, **29a-d** and **30a-d**.

Table 2 SAR of C-4 substituted O-aryl analogs **39a-d**, **40a-d**, **41a-d** and **42a-d**.

Table 3 Antiangiogenic activity of representative compounds **17d**, **23d**, **29d**, **30d**, **39d**, **40d**, **41d** and **42d**.

Table 4. Docking energy scores in kcal/mol for the selected compounds in the active site of ER α and VEGFR-2

Compound	CDOCKER Interaction Energy (ER α)	CDOCKER Interaction Energy (VEGFR-2)
17d	-68.14	-52.46
23d	-57.67	-49.59
29d	-57.78	-53.23
30d	-58.31	-52.19
39d	-56.92	-52.09
40d	-58.64	-52.67
41d	-69.26	-55.13
42d	-67.25	-53.73

Highlights

- A series of coumarin-based analogs were rationally designed and synthesized.
- **42d** inhibited cancer cell proliferation and migration as well as angiogenesis.
- Synergetic effect of **42d** on ER α and VEGFR-2/Raf-1/MAPK/ERK pathway.
- **42d** turned out to be a promising dual targeting candidate for breast cancer.